JPRS-UEQ-93-001
29 January 1993

JPRS Report

Science & Technology

Central Eurasia: Engineering & Equipment

Science & Technology

Central Eurasia: Engineering & Equipment

JPRS-UEQ-93-001 29 January 1993

CONTENTS

NUCLEAR ENERGY

NON-NUCLEAR ENERGY

MECHANICS OF GASES, LIQUIDS, SOLIDS

INDUSTRIAL TECHNOLOGY, PLANNING, PRODUCTIVITY

Efficiency of Jet Descending Module Braking Methods in Planetary Atmospheres

937F0069A Moscow VESTNIK MOSKOVSKOGO GOSUDARSTVENNOGO TEKHNICHESKOGO UNIVERSITETA: SERIYA MASHINOSTROYENIYE in Russian No 2, Apr-Jun 92 pp 19-28

[Article by V.T. Kalugin, A.Yu. Lutsenko, A.A. Afanasyev; UDC 533.6.011]

[Abstract] Attempts to find optimum methods of controlling the aerodynamic characteristics of spacecraft (LA) capable of operating under all motion conditions both in rarefied and dense media necessitated an investigation into the use of jet-type control systems (SOU), particularly for controlling the descent module flight in the atmospheres of planets. The shortcomings of existing retroengines (TDU) which are a version of jet-type flight control systems but interfere with the external flow about the descent module (SA) airframe prompted a study of the efficiency of jet-type methods of decelerating the descent modules and simulating the interaction of the external uniform flow with the jet-module system. The results of aerodynamic studies of various jet deceleration methods are cited, characteristic features of jet flows are considered, feasible ranges of aerodynamic characteristics are indicated, and flow stability ranges are identified. The study specifically addresses segmented-conical descent modules. Formulae are derived for calculating the drag force and thrust coeffifcient. The findings show that the greatest aerodynamic interference under a jet interaction occurs at a thrust coefficient of <3 where block and ring retrojet arrangements have advantages over a centrally positioned singe retroengine, yet block thruster arrangement is more suitable for control systems. Figures 5; references 2; 1 Russian, 1 Western.

Analysis of Hydrodynamic Indicators of Contraction Devices

937F0072A Moscow TYAZHELOYE MASHINOSTROYENIYE in Russian No 9, Sep 92 pp 23-25

[Article by E.Ye. Blagov, V.I. Chernoshtan, Ye.G. Vasilchenko, VNIIAM; UDC 621.646.2-5.001.8]

[Abstract] Restrictions, such as diaphragms, orifice plates, nozzles, and pipeline valves and their pressure loss which is the main characteristic of restrictions and is usually defined as the pressure differential between the inlet and outlet sections divided by the velocity head at the outlet section are discussed and it is noted that restrictions with an identical friction loss may differ significantly. This prompted an attempt to take into account the degree of pressure restoration in hydrodynamic analyses in the form of the cavitation onset coefficient in order to optimize the selection or design of restrictions whose hydrodynamic characteristics fit the best the specific operating conditions. The next step of hydrodynamic design optimization involves determining the relationship between the cavitation onset coefficient and a number of parameters determined by the flow section configuration. The total and static pressure profiles along the restriction channel are plotted and the empirical values of hydrodynamic flow indicators of various types of restrictions are summarized. An analysis of several types of restrictions makes it possible to draw the conclusion that the design conditions are realized in all cases of separating flows The findings make it possible to determine a number of important hydrodynamic indicators of restrictions. Figures 2; tables 1; references 10.

Examples of Evaluating Metrological Characteristics of Solid State Sensors for Subsatellite Systems

937F0068A Baku DOKLADY AKADEMII NAUK AZERBAYDZHANA in Russian No 3, 1990 [Signed to press 16 Jan 92] pp 41-44

[Article by I. M. Aliyev, M. G. Imranov, N. A. Mekhtiev, Yu. L. Feldman; UDC 681.586.326:(386:005):(629.786:528-855)]

[Text] The way the basic mean square root error of sensors on platforms for a nature space exploration system is determined is by doing an approximate calculation based on statistical data of the sensor's sensitivity to various impacting factors. Therefore, of real interest is the development of a technique for determining whether the evaluations of error which are obtained correspond to the real errors in measuring the appropriate physical parameters on these platforms (1-5).

By definition, the basic root mean square error for the device and for the measurement results should agree numerically. This requirement stipulates the route which must be taken when searching for evidence that the technique chosen for determining the basic root mean square error was the correct one (4).

In most cases, this technique is a physical modelling process of the operating conditions of the sensor on the platform. All impacting factors present on the platform are naturally occurring on the given platform and exist in those combinations of strengths typical for that platform. By measuring a physical parameter whose values are close to those which really exist on the platform at each moment in time, and which are also known fairly accurately, we can account in the correct ratios for how error is affected by the outcome of measuring additive and multiplicative sensitivities of the given sensor being researched. Thus, this technique makes it possible to check in a comprehensive manner that the adopted assumptions are correct, as well as the performance of the proposed mathematical model of the basic root mean square error as a whole (3).

If there is a marked deviation (by 30-50%) between the obtained actual basic error and that calculated, it is

necessary to determine the reason for these deviations. Reasons for the observed discrepancy may be the following:

1. A discrepancy in the calculated value of the scale use coefficient to its actual value for the given platform. A check is performed by using the measurement data of the auxiliary sensor. For all these data, the mathematical expectation of the magnitude of the measured parameter is found first, and then the coefficient of scale use is found by using the measurement limit of the sensor being researched.

2. A discrepancy in the laws of distribution of the impacting factors present on the platform to their previously obtained statistical models. A check is carried out by installing additional sensors for all the impacting factors on the platform and repeating the research cycle.

3. A discrepancy between sensitivities of the sensor being researched to the impacting factors and the values in the data sheet. A check is carried out by repeating the certification of the sensor after the research cycle is over.

4. A discrepancy between the a priori adopted mechanism for adding the components of error due to the influence of the impacting factors and the real mechanism for forming the basic root mean square error. This is checked by researching the magnitude of the mathematical expectation of the error in the array of measurement results obtained from the sensor being researched. The presence of systematic error in all the measurement results and the compatibility of this error with the root mean square error value is indicative of the fact that all measures to eliminate systematic components of error have not been taken on this platform, and the way the sensor is used on the platform must be modified.

When this technique is actually being used, the most difficult aspect is creating a highly accurate stimulus of the measured physical parameter. This stimulus should be capable of functioning under the conditions existing on the given platform or the object being researched from it. However, since such stringent requirements for rapid action are not placed on such a stimulus, if rapid action of the stimulus is exchanged for accuracy, a technical solution to the task can be found in the overriding majority of cases (4).

In this work, approving the technique for checking the conformity of the calculated and determined metrological characteristics of the sensor in the experiment was carried out on sensors with various physical parameters. Common to all cases was the conversion of the signal from the auxiliary sensor into a digital code, an approximation of the obtained value of the code to the standard code values which are closest to it and which correspond to the fixed parameter level, and the recording of all information signals on the recorder, also in digital code (3).

For the magnetic field voltage sensor, this technique can be performed in the simplest way, since creating a magnetic field with the appropriate voltage is a relatively easy task. The unit for carrying out the research is a board with two sensors and an electromagnetic field exciter coil. The sensor being researched was placed in the zone of the uniform magnetic field of the exciter. Around the exciter and the sensor being researched, a three layer magnetic screen was placed. The screen was made out of soft magnetic material. The screen was perforated to equalize the temperature fields within the screen and around it.

The exciter was powered from a stabilized, regulated DC power source, controlled by the code input. From the sensors (those being researched and control sensors), signals were converted into digital code with an analog-to-digital converter operating using the dual integration technique with weighting function. This allowed the 50 Hz commercial frequency interference to be effectively suppressed during the measurement time which was somewhat longer than 100 milliseconds.

Using this technique, a check of the sensors showed the following.

1. for land-based and offshore platforms, systematic error values were obtained for various sensors within a range of 0.12% to +0.027% with an average basic root mean square error value of approximately 0.5%, which indicates that the adopted error model was correct.

2. the real root mean square error of the measurement results for the batch of sensors was within the range of 0.54% to 0.58% for the land-based platform (calculated value of 0.6%) and within the range of 0.39% to 0.44% for the offshore platform (calculated value of 0.47%), which indicates a good correspondence between the calculated data and those found by experiment for evaluating the quality of the sensors.

For the infrared source energy brightness sensor, the research conditions were somewhat complicated, since it was necessary to provide a connection between the plane or helicopter platform on which the infrared radiation sensor was mounted and the exciter located at the test location. In other respects, the task was resolved in much the same way. Using an ultra shortwave channel of radio communication allows all the necessary information to be stored on the recorder of the observation land-based station. As an exciter of infrared radiation, an electric heater with a flat heat exchange element two meters square was used.

The results of this research showed that the proposed technique for determining the basic error gives sufficiently close results for the majority of the sensors used (discrepancies between the calculated and observed values of the basic error are not more than 0.4%). However, for the very same sensor, there are data arrays which are encountered that are outside the general statistical group. The systematic error for this data somewhat exceeds the root mean square value of error. Apparently, this is due to the fact that the additive

component from the action of mass impacting factors starts to dominate in a number of other components of the basic error.

For temperature sensors, the fuel element of a specially developed thermostat was the exciter. Testing was conducted on the land-based and helicopter platforms, but only in the region of positive temperatures. As a result of this, the data of this statistical research is not complete. At the present time, a thermocryostat is being developed to completely resolve the task (5).

However, the preliminary data obtained for the various types of temperature sensors do not contradict the adopted hypothesis that there is a correspondence between the calculated data and that obtained from the experiment.

Thus, an experimental check of the technique developed for determining the basic metrological characteristics of the sensor on various platforms showed its applicability for solving the indicated task.

Footnotes

1. T. K. Ismailov, "Developing Methods and Equipment for Subsatellite Observations," ISSLEDOVANIE ZEMLI IZ KOSMOSA [Researching the Earth from Space], 1980, No. 1, pp. 35-39.

2. I. M. Aliyev, M. G. Imranov, Yu. L. Feldman, "About One Analysis Method and Conclusions on the Informational Characteristics of Sensors for Aerial Space Systems to Research Nature," Space Research Scientific Production Association, Preprint No. 65, Baku, 1988.

3. I. M. Aliyev, N. N. Timoshenko, M. G. Imranov, D. B. Medzhudov, Yu. L. Feldman, "Some Issues about Rationally Constructing the Elements of Informational Measurement Systems for Remote Probing of the Earth," Azerbaydzhan Academy of Sciences, Series of Mathematics, Physics and Equipment, 1988, No. 4.

4. I. M. Aliyev, M. G. Imranov, N. A. Mekhniyev, Yu. L. Feldman, "The Possibility of Controlling the Informational Characteristics of Solid State Sensors for Subsatellite Systems," Reports of the Space Research Scientific Production Association, Baku, 1989.

5. N. D. Gadzhiyev, "Solid State Converters of Non-Electric Values based on Microelectronic Technology for Subsatellite Systems," Theses of Science, Moscow, 1985.

Holographic Lateral Displacement Interferometer

937F0078A St. Petersburg OPTICHESKIY ZHURNAL in Russian No 4, Apr 92 pp 3-7

[Article by V.G. Gusev, Tomsk State University; UDC 778.38:681.787]

[Abstract] A holographic lateral displacement interferometer for monitoring the wave front using diffuse scattered fields in which the defocusing magnitude is determined solely by the alignment error is considered; this interferometer is specifically intended for lens and objective lens quality control. The double exposure holographic optical recording and restoration procedure involving spatial filtering in the far field diffraction zone is outlined. A frosted screen is illuminated by a converging spherical wave with a radius of curvature equal to the focal length of the lens and the hologram is recorded during the first exposure; before the second exposure the frosted screen and controlled lens are displaced laterally and perpendicularly to the optical axis. The spatial filtering principle is described in detail and it is noted that the holographic interferometer has a number of advantages over known interferometers, e.g., those on the basis of holographic beam interferometry; it makes it possible to eliminate errors due to the optical imperfection of the component elements and perform field-based monitoring using a single hologram; moreover, the interference pattern is adjusted with the controlled objective lens pupil. The use of spatial filtering also makes it possible to separate a pattern which characterizes either axial or offset optical aberrations. Figures 4; references 10: 8 Russian, 2 Western.

Effect of Lower Light Beam Aberration Correction Accuracy on Beam Energy Transport Efficiency

937F0078B St. Petersburg OPTICHESKIY ZHURNAL in Russian No 4, Apr 92 pp 7-9

[Article by V.M. Buldakov, A.N. Glushkov, L.V. Streltsova, Astrofizika Scientific Production Association, Moscow and Atmospheric Optics Institute at the Siberian Department of Russia's Academy of Sciences, Tomsk; UDC 535.317.6:621.373.826]

[Abstract] The need to compensate for adaptive light signal distortions appearing during the beam generation and propagation in optical communication, ranging, and other areas and the issue of the wave front (VF) control and its correction accuracy are discussed and an attempt is made to analyze the effect of lower laser beam aberration correction errors on the transport efficiency of the energy concentrated in the beam. To this end, Strehl's number usually defined as the ratio of the mean field strength at a point in actual operation to its maximum value is used as an adaptive optics system operating quality characteristic. A formula is derived in order to find the dependence of the Strehl's number on the aberration correction accuracy in the case where the wave front aberrations and corrections are independent steady-state random processes. The effect of the focusing and aiming errors on the luminous energy transport efficiency is plotted and the condition is derived under which the fluctuation component of the aiming error has the principal impact on the Strehl number. The study shows that in the case of lower light beam aberration correction, effective energy transport calls for minimizing the focusing and aiming error. Thus, since the transport efficiency depends on the beam's width and spatial coherence, the requirements for the adaptive optical system accuracy characteristics must be imposed alloying for the values of these parameters. Figures 1; references 5.

Optical Radiation Phase Front Slope Measurement Error Analysis Using Hartman Transducers

937F0078C St. Petersburg OPTICHESKIY ZHURNAL in Russian No 4, Apr 92 pp 12-15

[Article by V.Ye. Kirakosyants, V.A. Loginov, V.N. Timofeyev, Astrofizika Scientific Production Association, Moscow; UDC 621.373.52]

[Abstract] The issue of measuring the radiation phase front (FF) of a distant source by placing a Hartman transducer array in the optical beam cross section and reproducing the entire phase distribution by measuring the phase front slopes is addressed. It is noted that the accuracy of such reproduction depends both on the algorithm governing the measurements and the slope measurement accuracy of individual transducers. The design and likely uses of the Hartman transducer are outlined and the principal outcome of a study of the accuracy with which the local slope (LN), mean slope (SN), and mean phase front derivative in the receiving aperture are measured is discussed. Two transducer design versions are considered—with a four-area photodetector and with a mosaic multichannel photodetector. The relationship between the values under study and the legitimate signal phase distribution in the transducer aperture is derived and the problem of analyzing the phase front slope estimates generated by the transducer is formulated. The effect of the random nature of the phase distribution in the receiving aperture and of the external noise which decreases the image contrast and complicates image processing on the transducer error is determined. It is shown that at low signal:noise ratios, both transducer design have similar errors while in the case of high ratios, the four-area detector measures the mean slope better while the mosaic one—the mean derivative. References 1

Algorithm of Spherical Mirror Calibration Using Three Interference Patterns

937F0078D St. Petersburg OPTICHESKIY ZHURNAL in Russian No 4, Apr 92 pp 16-18

[Article by V.B. Gubin, University of Friendship Among Peoples imeni P. Lumumba, Moscow; UDC 535.313]

[Abstract] The issue of spherical surface calibration with the help of three interference patterns using a Zerike polynomial series and calculating the mirror errors by approximating the interference patterns is addressed. It is noted that the problem can be solved more efficiently by using a modified basis in which the functions describing the sphere deformations are separated from the function describing only the sphere and beam offsetting contribution to the interference patterns. The three interference patterns involved in this certification method are considered in detail and it is shown that the interference pattern processing technique does not call for precise setting or knowledge of the mirrors' center of curvature positions relative to each other and the beam focus. The proposed calibration method is not absolute and the difference in the front errors at points symmetric in relation to the optical axis actually plays the role of a peculiar standard whose complex shape complicates its own calibration and makes it difficult subsequently to take its imperfection into account. Figures 2; references 4: 2 Russian, 2 Western.

Simulation of Binary Random Light Fields of Amplitude-Phase Screens

937F0078E St. Petersburg OPTICHESKIY ZHURNAL in Russian No 4, Apr 92 pp 18-21

[Article by V.F. Terzi, A.G. Konyukhov, Ye.N. Pavlov, State Applied Optics Institute, Kazan; UDC 621.383:621.397.3]

[Abstract] Attempts to simulate random absorbing and phase screens and random isotropic amplitude screens in order to simulate the optical transfer function (OPF) of such systems as the turbulent and scattering atmosphere are reported and numerous publications dealing with optical transfer function simulation by means of representing the functions as complex spatial filters (KPF) are reviewed. Simulation of random isotropic fields by representing them as a two-dimensional process and using multiple filtering recurrence to avoid the diagonal dependence is considered. The complex spatial filter transfer function encoding is examined and autocorrelation functions of various filters are summarized. An analysis shows that multilevel random fields may be used to derive the corresponding amplitude, phase, and amplitude-phase screens; the effectiveness of binary amplitude-phase screens can be increased by expanding the filter transmission band. The binary screen effectiveness is the same as that of multilevel fields and is approximately equal to 86% for 64x64 screens. Figures 2; tables 3; references 19: 4 Russian, 15 Western.

On Stability of Goniometric Instrument Elements' Optical Characteristics

937F0078F St. Petersburg OPTICHESKIY ZHURNAL in Russian No 4, Apr 92 pp 21-26

[Article by M.P. Kolosov, Geofizika Scientific Production Association, Moscow; UDC 681.786.3]

[Abstract] The mechanical, thermal, aging, and other factors which affect the optical elements (OE) of fixed-tuned and self-calibrating goniometers and upset their geometrical arrangement by deforming them and altering their optical characteristics which determine the angular position of the sighting line are discussed. For simplicity's sake, the effect of these factors on the optical element geometry is illustrated using the example of a simple prism or plate made as a parallelepiped whose edges are parallel to the corresponding axes of a rectangular system of coordinates; this prism is treated as a test element (TE) under the effect of a constant linear temperature gradient. The shape behavior of the element from one or several materials under various conditions and the quantitative estimate of the edge effect of optical materials (OM) are considered. The principal correlations between the physical parameters of optical materials and the optical characteristics of test elements are analyzed in detail and the principal relationship between the dimensional and optical characteristics are examined. It is noted that the above investigation is limited in scope and does not address such physical factors as anisotropy, temperature hysteresis, microdeformations due to a prolonged mechanical exposure, the discrepancy between the thermal expansion coefficients of thin coats and bulky bases, etc. Figures 3; tables 1; references 12: 11 Russian, 1 Western.

Wide-Angle Quartz Lyot Filter

937F0078G St. Petersburg OPTICHESKIY ZHURNAL in Russian No 4, Apr 92 pp 28-31

[Article by A.L. Aleksandrovskiy, T.A. Vinogradova, N.P. Depman, V.V. Tarasenko, Moscow State University and National Scientific Center at the State Optics Institute imeni S.I. Vavilov; UDC 535.345.67]

[Abstract] The advantages of Lyot and Sholz interference polarization filters (IPF) used in astrophysical and geophysical research and spectral analysis and laser ranging prompted an examination of the problems of making Lyo filters with large linear and angular apertures on the basis of synthetic quartz and a study of their optical properties. The operating principle of a Lyot interference polarization filter consisting of several stages, including a crystal birefringent plate sliced parallel to the crystal optic axis and placed between the polarizers, is considered. The quality criterion of an interference polarization filter intended for detecting a scattered signal

through angular noise with angular distribution and its principal parameters are examined and the spectral transmission of the interference polarization filter and interference filter (IF) and the angular dependence of the interference polarization filter transmission are plotted. The angular characteristics of the interference polarization filter, optical axis orientation in quartz slices, and polarizer characteristics are described in detail. The filter transmission depends primarily on the characteristics of the polarizers used. The component element parameters are optimized in order to enhance the legitimate signal emission. Figures 4; tables 1; references 9: 5 Russian, 4 Western.

On Effect of Surface Relief on Radiation Temperature of Bodies

937F0078H St. Petersburg OPTICHESKIY ZHURNAL in Russian No 4, Apr 92 pp 32-34

[Article by V.D. Mochalin; UDC 621.384.3:539.1.04]

[Abstract] The use of radiation temperature for determining the thermal condition of bodies and the lack of published data on the effect of the body surface relief on the radiation temperature (which is significant in a number of cases) prompted an investigation into the dependence of the radiation temperature on the observation and irradiation duration. To this end, a plate with cylindrical relief elements under natural heat exchange with the ambient medium is considered in the case where the element diameter does not exceed the infrared radiation detector's linear resolution and the surface is radiating diffusely. The effect of the bodies' surface curvature on their radiation temperature is addressed and the dependence of the radiation temperature of a plate and semicylinder on the observation and irradiation angles is plotted. An analysis demonstrates that the surface relief significantly affects the plate's radiation temperature under directional irradiation, e.g., solar radiation. Given a high thermal conductivity of the relief elements, e.g., metals, a decrease in the radiation temperature is largely due to to an increase in the effective convective heat transfer area. It is noted that in bodies with a poor thermal conductivity, the radiation temperature may vary by as much as 12-20K depending on the observation and irradiation directions. Figures 4; references 3.

Integral Optical System Quality Assessment Criterion

937F0073I St. Petersburg OPTICHESKIY ZHURNAL in Russian No 4, Apr 92 pp 34-37

[Article by I.L. Anitropova, V.A. Zverev, Leningrad Institute of Precision Mechanics and Optics, St. Petersburg; UDC 535.317.1]

[Abstract] The principle of optical image generation by means of distributing illuminance over a certain plane in the image space which is equivalent to the luminance distribution in the optically conjugated plane in the object space is considered and the concepts of energy capability of the optical system and its image quality which characterize the optical system quality are introduced. An attempt is made to derive a single expression for describing the quality of various types of optical systems, such as microscope objectives, achromatic and anastigmatic lenses, etc. It is noted that the possibility of expressing the integral quality estimate by a single number should be credited to E.H. Linfoot and that the proposed approach to assessing the optical system level can be formally applied to evaluating the image curvature correction in microscope objectives. References 9: 8 Russian, 1 Western.

Spherical Aberration Compensation in Mirror Optical System

937F0078J St. Petersburg OPTICHESKIY ZHURNAL in Russian No 4, Apr 92 pp 37-40

[Article by V.A. Semin, State Applied Optics Institute, Kazan; UDC 535.317.61]

[Abstract] The problem of compensating for the spherical aberration in mirror systems formed by spherical surface is considered and it is noted that thus far, the problem has been solved only for the case where the compensating aspherical surface which compensates for the total aberration of the remaining surfaces is located on the edge of the system. This constraint on the range of structures and other system capabilities prompted an attempt to solve the problem for the compensator position at any spot and not merely at the system edge. In so doing, only systems composed of coaxially positioned surfaces of revolution which are defined by meridional cross sections are considered. For illustration, a three-mirror system is examined in detail and it is noted that although today's computer system can solve the system simply by an exhaustive search of the profile equation, this method cannot always be used; direct solution is therefore suggested. The proposed equations can also be used for analyzing optical systems with aplanatic properties in addition to their axial astigmatism. Figures 2; references 4.

Finding Second Point of Beam Intersection With Respect to Second-Degree Nonclosed Surfaces

937F0078K St. Petersburg OPTICHESKIY ZHURNAL in Russian No 4, Apr 92 pp 40-41

[Article by D. Antonijevic, Novi Beograd, Yugoslavia; UDC 535.317:681.3]

[Abstract] An attempt is made to transform Feather's formulae used for analyzing on a computer the beam path in an optical system in order to find the second point of the beam intersection with the surface of a paraboloid of revolution or a hyperboloid. In particular, Feather's formulae are extended to the case where second-degree surfaces are used. The specific issue of finding the second point of intersection with a closed ellipsoid surface is also addressed. It is stressed that finding the far (i.e., second) point of intersection may be useful for analyzing the beam path through nonclosed surfaces with a single vertex, e.g., paraboloids and hyperboloids. Figures 1.

Spectrum Scanning Device

937F0078L St. Petersburg OPTICHESKIY ZHURNAL in Russian No 4, Apr 92 pp 41-43

[Article by Ye.D. Mishchenko, Yu.Sh. Akhunbabayev, St. Petersburg State University; UDC 681.785.5]

[Abstract] The increasing use of spectrum scanning devices and the effect of the scanning rate on their efficiency as well as the shortcomings of existing scanning method which is not suitable for operation at fixed wavelengths prompted the development of a special stepping motor for moving the parts of computer-aided spectrometric instruments. The use of the stepping motor in monochromatrors makes it possible to avoid mechanical wavelength meters or angle data transmitters since the motor has a discrete shaft rotation step and its angle depends linearly on a given number of steps. The proposed device makes it possible to accelerate the transition from one spectrum point to another which is necessary in operation at fixed points scattered over a broad range. The design and operation as well as optical train of the device are explained in detail. The new device was implemented in a pilot Luch-1 spectrometer produced at the Leningrad Optics-Mechanics Association (LOMO). Its use makes it possible to shorten the specified wavelength setting time in sequential spectral analysis by approximately a hundred fold. Figures 1; references 4.

Liquid Crystal Light Modulators With Fiber Optic Frontal Window

937F0078M St. Petersburg OPTICHESKIY ZHURNAL in Russian No 4, Apr 92 pp 44-47

[Article by B.G. Aleksandrov, M.V. Isayev, I.I. Kuzmina, V.V. Nikitin, A.P. Onokhov, National Scientific Center at the State Optics Institute imeni S.I. Vavilov and National Scientific Research Institute of Television, St. Petersburg; UDC 535.241.13]

[Abstract] The expanding used of space-time light modulators (PVMS) and correlators based on a photoconductor-liquid crystal (FP-ZhK) structures with a fiber optic frontal window and the relatively high quantum efficiency of the $As_{10}Se_{90}$ chalcogenide glassy semiconductor photolayer at a 633 nm wavelength which limits the image brightness amplification in space-time light modulators employing He-Ne laser radiation for reading as well as the limited operating life of such devices prompted the development of a space-time light modulator on the basis of thin ZnSe films which are transparent to the reading light with a wavelength of 500 nm or more and in which the dielectric mirror is removed beyond the photoconductor-liquid crystal structure. The design and operating principle of pilot samples of the new device are outlined and the dependence of the STLM transmission (i.e., its electrooptical response) in crossed polarizers on the exciting radiation intensity due to the hybrid and S-effect at various power supply voltage amplitudes and the energy spectrum of spatial noise of various structural elements are plotted. An analysis of the sensitivity, resolution, spatial noise level, and response speed of the STLM confirms the efficiency of optically controlled liquid crystal structures with high reflected light modulation parameters and demonstrates that their possibilities have not been exhausted. The outlook for using the new STLM for entering images into analog coherent optical computers as well as high-resolution adaptive optics elements is assessed. Figures 3; references 7: 6 Russian, 1 Russian.

Computer-Aided Optoelectronic Roughness Indicator

937F0078N St. Petersburg OPTICHESKIY ZHURNAL in Russian No 4, Apr 92 pp 51-53

[Article by B.D. Borisov, P.S. Golubev, A.S. Mishnev, Laser Physics Institute at the Siberian Department of Russia's Academy of Sciences, Novosibirsk and Design Engineering Institute at the Siberian Department of Russia's Academy of Sciences; UDC [531.717.2: 621.383.4'3]:681.3]

[Abstract] The need for combining the function of an optical micrometer with scanning along a certain coordinate for measuring the surface roughness prompted the development of a multichannel optoelectronic device with a simple optical train and standard multielement photodetectors. It utilizes a noncoherent light source with a light-shade boundary projection upon a 1200 TsL2 precision linear charge coupled device (PZS) photodetector. The optical design of the new device and its operating principle are outlined in detail and the following specific features are noted: it can take measurements of both absolute values and deviations accurate within 12 μm or better (using interpolation) within the measurement zone while the outcome does not depend on the sample position within the zone; it does not call for preliminary zero calibration when changing the product of sample; it can be used for measuring products with a size or deviation larger than the CCD ruler aperture. The specifications of the device are summarized and it is noted that it can be used for dimension inspection of tubes and rolled products with a complex shape. Figures 3; tables 2; references 6: 5 Russian, 1 Western.

Absorption in Interference Coats of Industrial CO_2 Laser Optical Elements

937F0078O St. Petersburg OPTICHESKIY ZHURNAL in Russian No 4, Apr 92 pp 56-58

[Article by V.N. Glebov, A.M. Malyutin, V.P. Yakunin, Scientific Research Center of Industrial Lasers at Russia's Academy of Sciences, Shatura; UDC 621.373.826.038.8]

[Abstract] The importance of minimizing absorption losses in such optical transmission elements of industrial CW CO_2 lasers with a radiating power of over 1 kW and

high radiation quality as mirrors and windows and the difficulty of producing and applying interference coats to optical elements (OE) prompted a study of absorption of 10.6 μm radiation of such half-wave coats on KCl substrates. The study is performed by the laser calorimetry method whereby the coats are produced by chemical vapor deposition in a vacuum using the coat-forming materials (POM) traditionally used in the infrared spectrum. KCl was selected as the substrate material due to its low volumetric absorptance and the possibility of producing surfaces free of contamination, e.g., by spalling. The dependence of the total absorptance of a freshly spalled 4-5 mm KCl slice on the total height of the steps in the spalling is plotted. The half-wave layers are applied by resistive and electron beam evaporation in a BAK-600 unit made by BALZERS. Coat-forming materials manufactured by various enterprises are examined and the spectral response of single layers is analyzed in a 4,000-5,000 cm^{-1} range using a Perkin-Elmer PE-983 spectrophotometer. The coats types, materials, manufacturers, deposition methods, chamber pressure, deposition rate, layer absorption and refractive index, and half-wave layer absorption are tabulated. The findings made it possible to develop highly reflective cavity mirrors on Ge substrates with a reflectance of at least 99%, transmittance of 0.2-0.5%, and absorptance of no more than 0.5%. They are currently used in industrial CO_2 lasers developed at the Scientific Research Center of Industrial Lasers at Russia's Academy of Sciences. Figures 1; tables 1; references 6: 2 Russian, 4 Western.

Producing YBaCu Layers for Superconducting Bolometers

937F0078P St. Petersburg OPTICHESKIY ZHURNAL in Russian No 4, Apr 92 pp 58-62

[Article by I.I. Shaganov, O.P. Konovalova, M.B. Krayukhin, A.D. Tkachenko, I.A. Khrebtov, National Scientific Center at the State Optics Institute imeni S.I. Vavilov; UDC [621.315.5:538.945]:539.216.2]

[Abstract] The issues of developing thin high-T_c superconducting (VTSP) layers, particularly by thermal vapor deposition and ion plasma spraying (IP), are addressed and these processes are divided into two categories: coprecipitation or cospraying and layer-by-layer or sequential deposition. The specific advantages of depositing alternating layers onto a HTSC substrate, especially the possibility of using standard vacuum equipment, prompted the development of new practices of producing YBaCu layers using a BU-1A commercial vacuum unit intended for making multilayer optical coats by the methods of resistive and electron beam evaporation. The new procedure is based on successively depositing specific Y, Ba, and Cu layers, ensuring their 1:2:3 stoichiometric ratio. A diagram of the crystallizing-oxidizing sample annealing in making YBaCu layers by sequential deposition, the relative surface resistivity of the layers near T_c, the effect of high-temperature annealing on the properties of YBaCu layers on aluminum oxide with a ZrO_2 buffer layer, and the temperature dependence of a strip element resistance are plotted. Crystallizing-oxidizing annealing significantly affects the T_c behavior, making it possible to speculate that the T_c values can be controlled within a 77-85K range. Potential uses of YBaCu layers on sapphire substrates in cryoelectronics are noted. Estimates show that a HTSC antenna bolometer on a sapphire crystal may have a time constant on the order of 10^{-9} s. It is also speculated that excess $1/f$ noise inherent in polycrystalline films will not limit the bolometer sensitivity threshold at high modulation frequencies. Figures 4; tables 1; references 11: 5 Russian, 6 Western.

Analytical Method of Determining Rough Diamond Grinding Process Elements Alloying for Machine Tool Kinematics

937F0078Q St. Petersburg OPTICHESKIY ZHURNAL in Russian No 4, Apr 92 pp 62-66

[Article by V.V. Travin, L.D. Ptitsyna, National Scientific Center at the State Optics Institute imeni S.I. Vavilov; UDC 681:7.053.35:681.7]

[Abstract] Rough diamond grinding using diamond wheels and machine tools with various tool kinematics and different tool spindle positions in relation to the product spindle at the zero reading is discussed and specific machine tools manufactured domestically as well as in Belgium, Germany, and France are mentioned. The mechanical diagrams of machine tools with different working feed direction are described in detail. In particular, the working feed direction along the product spindle axis, working feed direction along an arc of a circle at a 15° angle to the product spindle axis, and working feed direction along the tool spindle axis are considered. The advantages and shortcomings of the three methods for polishing surfaces of various shapes are examined and recommendations are made for selecting the specific arrangement in each case. Figures 4; references 4.

Optical Properties of Plastically Deformed Leucosapphire

937F0078R St. Petersburg OPTICHESKIY ZHURNAL in Russian No 4, Apr 92 pp 53-55

[Article by N.L. Sibikina, I.I. Afanasyev, L.I. Belevtseva, V.N. Petrov, B.A. Ignatenkov, A.P. Kiselev, National Scientific Center at the State Optics Institute imeni S.I. Vavilov; UDC 548.55:539.37]

[Abstract] The use of high-temperature plastic deformation of discs with central-circular bending for making meniscus blanks of *z*-sections of leucosapphire and the advantages of this method are discussed and it is noted that the conoscopic cross deviates from the microconoscope center. An attempt is made to measure the optical axes deviation of the corresponding radial directions in

the leucosapphire meniscus. To this end, menisci made by plastic deformation with central-circular disc bending from leucosapphire italz-sections by the State Optics Institute (GOI) methods are studied. A special sample holder is made for the Stoc goniometer, making it possible to align the meniscus center of symmetry with the point of intersection of the meniscus optical axis and the goniometer rotation axis. The microconoscope pattern on the meniscus surface and the diagram of the goniometer with the sample holder are cited and the angular distribution of the optical axes relative to the spherical meniscus radii is plotted. An analysis from the crystal optics viewpoint confirms the possibility of making optical elements with new properties whereby the optical axis deviation from the normal at each spherical meniscus surface point does not exceed 2.5°. This unique property may be used to develop lenses and menisci for short wave radiation. Figures 3; references 3: 2 Russian, 1 Western.

Error Analysis of Goniometer With Quasiperfect Coordinate System

937F0078S St. Petersburg OPTICHESKIY ZHURNAL in Russian No 4, Apr 92 pp 47-51

[Article by V.A. Meytin, Krasnaya Gora Optical Plant; UDC 681.786.3]

[Abstract] The errors of a goniometer with a quasiperfect coordinate system and altazimuth or equatorial mounting equipped with mirror-prismatic coordinate system mec.a (ZPNSK) are analyzed and the effect of the position indicator and tube errors is examined. To this end, an attempt is made to find the mathematical expectations which make it possible to calculate the instrument accuracy and select the tolerances for its principal structural members. Each error is regarded to be random and independent; on this basis, the standard deviation of the sighting direction measurement is found. The goniometer error and expectation expressions make it possible to determine the component element tolerance under various operating conditions. Figures 2; references 2.

Role of Frictional Forces in Grinding and Polishing of Optical Elements in Machine Tools Operating by Lapping Method

937F0078T St. Petersburg OPTICHESKIY ZHURNAL in Russian No 4, Apr 92 pp 66-70

[Article by Yu.V. Ashkerov, Scientific Research Institute of Higher Education, Moscow; UDC 681:7.053.45: 531.43]

[Abstract] The lack of data on the issue of friction and lubrication with respect to grinding and polishing of optical elements and the need to understand the complex physical and chemical processes under whose effect the optical surface is formed prompted an investigation into certain aspects of this problem. In particular, a rheological model of a diamond polishing tool based on the Voight-Kelvin model consisting of a spring and a damper assembled parallel to each other and a model based on the Maxwell model consisting of a damper and a spring connected in series are considered. A chain of abrasive grains with alternating masses is separated from the chaotically positioned abrasive grains in the binder and a deterministic equation of the particles' frequency is formulated and solved. An analysis of the motion equation of the chain mass in the tangential and normal directions shows that that there is no energy transfer among the diamond grains in the Maxwell model. The effect of the frictional forces on the diamond grain vibrations which, in turn, affect the optical surface quality is examined and the behavior of the friction coefficient under various polishing conditions is plotted. Characteristic oscillograms of the polishing and grinding force components in the normal and tangential directions make it possible to attribute the frictional force behavior to a change in the slope of the dropping dependence of the friction coefficient on the particle velocity. It is noted that the system vibrations under various friction conditions can be analyzed more fully only using simulation and computational experiments. Figures 4; references 17.

Determining Statistical Image Characteristics of Polished Metal Surfaces

937F0077A St. Petersburg OPTICHESKIY ZHURNAL in Russian No 3, Mar 92 pp 3-7

[Article by I.S. Melnik, Kiev Polytechnic Institute; UDC 681.2:669.058.001.57]

[Abstract] A metal surface image model and an expression for the two-dimensional autocorrelation function (AKF) cross section derived earlier (see *OMP* No 6, 1982) are discussed and it is noted that they do not fully reflect the specifics of individual field elements. A procedure of determining the statistical characteristics (the autocorrelation function and Wiener-Khinchin spectrum) of polished metal surfaces on the basis of their known models allowing for the effect of such diverse defects as circles and strips is considered. The procedure of calculating the statistical characteristics is presented and the autocorrelation function normalization of the polished metal surface model and experimental autocorrelation functions are plotted. An experimental verification of the analytical procedure is carried out by scanning a polished metal surface with a photodetector and a slotted diaphragm and an experimental unit block diagram is cited. Two types of autocorrelation function are identified—rapidly dropping and slowly decreasing; two distinct segments are also identified in the Wiener-Khinchin spectrum—low- and high-frequency. The findings show that extended linear elements in the image lead to an autocorrelation function expansion to correlation ranges commensurate with the mean scratch length on the surface. The expressions in the study describe the autocorrelation function and the energy

spectrum more accurately within the entire correlation interval range and spatial frequency band and may be used for analyzing the signal of image converters which scan polished surfaces. Figures 4;tables 1; references 7.

On Analyzing Weak Signal Detection Characteristics in Laser Ranging Tasks

937F0077B St. Petersburg OPTICHESKIY ZHURNAL in Russian No 3 Mar 92 pp 7-10

[Article by V.D. Chuvashov, S.N. Shapovalov, National Scientific Center at the State Optics Institute imeni S.I. Vavilov; UDC 621.396.967]

[Abstract] Limited applications of the so-called direct detection or photon counting method for estimating the actual capabilities of weak signal detection systems in laser detection and ranging tasks and the inexpediency of using the range equation in its canonical form prompted an attempt to assess the effect of angular fluctuations of the laser range finder's (LL) radiation pattern (DN) on the optical signal detection characteristics allowing for the discrete structure of the signal and noise being received. These detection characteristics are analyzed under the following assumptions and conditions: optical radiation is detected by counting individual photoelectrons; the total noise due to the background exposure and photodetector dark current is Poisson-distributed; the laser range finder radiation pattern is Gaussian; the detector operate threshold is determined by the Neumann-Pierson criterion; the angular beam pattern fluctuations are normally distributed; and the target is assumed to be a point target. The dependence of the correct detection probability on the absolute signal level for specular and rough surfaces and the dependence of the correct detection probability on the signal:noise ratio are plotted. The proposed procedure may be used both for assessing the performance of actual systems and for optimizing such parameters as the laser range finder beam width. Figures 2; references 4.

Use of Pyrodetectors in Double-Beam Balanced Photometers

937F0077C St. Petersburg OPTICHESKIY ZHURNAL in Russian No 3, Mar 92 pp 14-16

[Article by I.A. Bublichenko, Moscow Engineering Physics Institute; UDC 681.785.4]

[Abstract] The effect of optical signal fluctuations at the beam switching moment on the zero reading drift of classical double-beam balanced photometers with a single photodetector (FP) instrument is discussed and it is noted that the use of synchronous detection (SD) makes it possible to approach the selection of electronic noise suppression facility design from a unified viewpoint and limit the analysis by considering channel switching without dark intervals. The possibility of increasing the synchronous detection efficiency by "cutting out" the switching moment with the help of pyroelectric radiation detectors whose transmission band has a lower bound due to the nature of pyroelectricity and due to their design features is investigated. The frequency dependence of the voltage sensitivity of a PM-5 pyrodetector, a differentiator without and with low-frequency equalization, and photodetector with and without low-frequency equalization are plotted. The procedure made it possible to decrease the zero drift of a gas analyzer photometer to a level observed only in laboratories, i.e., 2×10^{-3} which corresponds to an ethylene concentration of 8×10^{-5}%. Gas analyzer tests conducted over four seasons confirm the high reliability of its photometer and photodetector. Figures 3; references 12: 11 Russian, 1 Western.

Photoelectric Device Response During Recording of Light Scattered by Elongated Particles

937F0077D St. Petersburg OPTICHESKIY ZHURNAL in Russian No 3, Mar 92 pp 16-18

[Article by I.P. Kudreyko, Physics Institute imeni B.I. Stepanov at the Belarussian Academy of Sciences, Minsk; UDC 53.082.52]

[Abstract] The use of photoelectric recording of the variation in the signal incident upon a flow of particles successively passing through the volume under study in order to monitor the granulometric composition of a disperse medium, particularly the use of a cylinder model for describing elongated particles and plotting their calibration curve, is described and an attempt is made to evaluate the magnitude of the signal entering the round photodetector when radiation is scattered by a highly elongated particle with a random orientation whereby the incident radiation is shaped as a cone with an apex on the particle axis. The problem is formulated geometrically and scattering on an infinite cylinder is graphically represented due to the fact that the problem is solved using an infinitely long cylinder approximation. The dependence of the signal magnitude on the angle between the symmetry axes of the incident beam and the detector aperture in a plane perpendicular to the cylinder axis is plotted. The findings show that at equal radiation detection solid angles, the signal entering a rectangular aperture is greater than the signal entering a round aperture. The formulae derived in the study make it possible to analyze on-line the photoelectric counter's response to radiation scattered by a highly elongated particle in a round aperture with a random focused light beam incidence. Figures 3; references 4: 3 Russian, 1 Western.

Method of Mechanical Sine Light Modulation

937F0077E St. Petersburg OPTICHESKIY ZHURNAL in Russian No 3, Mar 92 pp 19-21

[Article by A.V. Lenskiy, Astronomical Observatory at the Kiev State University; UDC 535.311]

[Abstract] The use of sine luminous flux modulation in studying the time response to incident radiation and the importance that the modulator not limit the so-called geometrical factor, i.e, the product of the beam cross section at the transmission peak in the modulator by the solid angle within which the luminous flux propagates, are discussed. The possibility of realizing simple mechanical light modulation whereby the sine shape does not depend on the geometrical factor, i.e., can be obtained at any given real value of either the area or angle, is investigated and the luminous flux modulation principle is considered analytically and graphically. It is shown that Fourier series of the periodic piecewise-linear function characterizing the luminous flux modulation does not contain harmonics whose number is divisible by 3. The proposed sine modulation principle does not impose any practical constraints on the area and angle. Moreover, the diaphragm illuminance must remain constant only in one direction, thus expanding the range of light sources used and simplifying the optical train as well as making it possible to simultaneously modulate light at various wavelengths even if the modulator operates at a spectrometer output. Figures 1; references 5: 2 Russian, 3 Western.

Heat Source Power Fluctuations During Propagation in Turbulent Atmosphere

937F0077F St. Petersburg OPTICHESKIY ZHURNAL in Russian No 3, Mar 92 pp 22-24

[Article by G.M. Samelson, Telecommunications Institute imeni M.A. Bonch-Bruyevich, St. Petersburg; UDC 551.593:681.7.069]

[Abstract] Intensity fluctuations at the reception point as a result of propagation in a turbulent atmosphere and the task of intensity fluctuation decorrelation of various spectral radiation components after propagation in an atmosphere, especially for explaining certain stellar scintillation patterns, are considered. In so doing, the problem is solved in the case where the spectral variance can be ignored. This formulation makes it possible to evaluate the relative effect of phenomena of various origins on the variance and is also valuable for examining the impact of thermal source twinkling in the infrared spectral windows or over horizontal or close-to-vertical paths in the visible spectrum on the adaptive optics system performance. To this end, monochromatic radiation is studied. An analysis of the expression for the relative integral power fluctuation variance shows that the variance is a function of the parameters which characterize the relative dimensions of the source and the receiving aperture and also depends on the path geometry and turbulence intensity which is assessed by a generalized parameter. It is noted that *a priori*, the findings do not take into account the atmosphere's spectral variance and their applicability is limited to the area of weak fluctuations. Tables 1; references 11: 7 Russian, 4 Western.

On Possibility of Theoretically Analyzing Frequency-Contrast Characteristic of High-Definition Cathode Ray Tube Screens

937F0077G St. Petersburg OPTICHESKIY ZHURNAL in Russian No 3, Mar 92 pp 25-27

[Article by V.B. Mikhaylik, V.I. Pigrukh, N.S. Pidzyraylo, Lvov State University and Erotron Design Office; UDC 621.385.832:621.757]

[Abstract] The relative role of the frequency-contrast characteristic (ChKKh), cathodoluminescence energy yield, interelement luminance variation (MNYa), and contrast gain (KPK) of the cathodoluminescent screen (KLE) of cathode ray tubes (ELT) in determining the CRT quality and definition is discussed and the lack of practical procedures for quantifying the cathode ray tube quality is noted. An attempt is made to develop a physical-mathematical model which describes the image generation on the cathodoluminescent screen and correlate its conclusions with the results of gain measurements. To this end, the frequency-contrast characteristic analysis method based on the theory of diffuse approximation of radiant energy transport equation in a disperse layer is selected for solving this problem as being the most realistic. The relative simplicity and uniqueness of the proposed expression for the frequency-contrast characteristic of the cathodoluminescent screen and the possibility of experimentally determining all initial parameters necessary for calculations are taken into account. The screen surface profile and the dependence of the contrast gain of a sample screen on the ratio of the spatial frequency to the commercial CRT resolution, i.e., frequency-contrast characteristic, are plotted. The analytical procedure for ZnS:Ag and Y_2SiO_6Ce phosphor makes it possible to determine with sufficient precision the transfer properties of fine thin cathodoluminescent screens and may be quite useful for understanding the physical nature of the image generation and transmission process and for predicting the possibility of further improving the CRT screen quality. Figures 2; tables 1; references 15: 12 Russian, 3 Western.

Study of Reflex Camera Viewfinder Focusing Accuracy

937F0077H St. Petersburg OPTICHESKIY ZHURNAL in Russian No 3, Mar 92 pp 28-30

[Article by E.V. Babak, A.V. Gitin, V.A. Fedorov, National Scientific Center at the State Optics Institute imeni S.I. Vavilov and Precision Mechanics and Optics Institute, St. Petersburg; UDC 681.7.013.8:771.371.5]

[Abstract] The shortcomings of the frequency-contrast characteristic (ChKKh) method and Schade's equivalent frequency width method which prevented them from being unified into a procedure of monitoring the focusing accuracy of a reflex camera viewfinder as the emergence of laser focusing screens with synthetic indicatrices which make the viewfinder focusing accuracy monitoring task especially acute prompted a study of this

issue. A schematic diagram of a unit developed for measuring the image sharpness is cited and a defocusing curve of the reflex camera model is plotted. The study utilizes a family of experimental frequency-contrast characteristic curves which are assumed to be known. A viewfinder model of a reflex camera with a collecting lens from a Zenit Ye camera and an objective lens of a Gelios-44M camera is used. The method may be used to examine the effect of the optical characteristics of the frosted focusing screen—both the indicatrix and surface structure regularity—on the viewfinder focusing accuracy. Figures 3; references 7: 5 Russian, 2 Western.

New Frustrated Total Internal Reflection Prism Elements

937F0077I St. Petersburg OPTICHESKIY ZHURNAL in Russian No 3, Mar 92 pp 30-33

[Article by V.B. Yakovlev, National Scientific Center at the State Optics Institute imeni S.I. Vavilov; UDC 681.7.065:543.422]

[Abstract] The theoretical difficulties characterizing the synthesis of optical systems with frustrated total internal reflection (NPVO) due to the fact that crystal morphology is barely suitable for predicting the shape of optical elements, the limited heuristic value of existing methods of solving this problem, and the general importance of FTIR technology prompted the use of the system morphology method for synthesizing FTIR elements, particularly direct vision prisms which make up the component base of the PIK and PUVI adapter series widely used since 1980. The element shape is synthesized by a lower-order subsystem (PS) convolution into higher-order systems with subsequent physical and geometrical interpretation and duplication with the help of symmetry operations. To this end, Amici (Dove), Abbe, Newton, Hummel, and new prisms are considered and the transmission curve of a ceramic prism used in a Perkin-Elmer 1700 Fourier-spectrometer and infrared spectrum of a polyethyleneterephthalate (PETF) film produced in a UR-20 unit with the help of a PIK-388 adapter with the same ceramic prism are plotted. The use of the theoretical tools of geometrical synthesis of FTIR optical elements makes it possible to develop new types of reflecting prisms with improved technical characteristics compared to existing prisms. An experimental check confirms the good performance of the new optical ceramic prism. Figures 4; references 12.

On Quality of Light Beam Formed by Composite Aperture

937F0077J St. Petersburg OPTICHESKIY ZHURNAL in Russian No 3, Mar 92 pp 33-35

[Article by V.Ye. Kirakosyants, V.A. Loginov, V.V. Slonov, Astrofizika Central Design Office, Moscow; UDC 681.7.013.22:535.241.44]

[Abstract] The effect of the possibility of laser radiation focusing with the help of a transmitting optical system, i.e., its dimensions and fabrication precision, on the efficacy of optical communication and range finding tasks and the issue of the sectional aperture element installation accuracy—the alignment of smaller subapertures forming a large sectional aperture—prompted an investigation into the quality of the light beam formed by such a sectional aperture. The mean axial radiant intensity in the recording plane, i.e., the simplest quality criterion, is derived through the values of Strehl's numbers and the positioning computation errors of the composite aperture elements are summarized. An analysis shows that Strehl's number is determined by the distance between the subapertures and does not depend on other parameters characterizing their mutual position. The accuracy of the analytical formulae derived for assessing the quality of radiation formed by the sectional apertures is quite adequate, at least at small positioning errors. Tables 2; references 3.

Efficiency Estimate of Infrared Imaging Equipment Utilizing Polarization Contrast of Objects

937F0077K St. Petersburg OPTICHESKIY ZHURNAL in Russian No 3, Mar 92 pp 35-37

[Article by R.M. Aleyev, V.A. Ovsyannikov, State Applied Optics Institute, Kazan; UDC 621.384.326]

[Abstract] The polarization contrast of objects which is due to the difference in their emissivity for radiation components polarized in the plane of radiation leaving the object surface and in a perpendicular plane is one of the characteristic features which can be used for expanding the capability of infrared imaging equipment (TVA). A polarization contrast formula is derived and an attempt is made to develop a procedure to assess the efficiency of an infrared imaging device utilizing the polarization contrast phenomenon for target detection. To this end, the effect of the environment on the radiation polarization is examined in the case where the target is observed through an atmospheric layer with a given transmission within the observation wavelength range. For illustration, the degree of target radiation polarization with an unknown polarization azimuth is determined using a four-element photodetector with polarizers in front of each element. The relative detection threshold for the polarization contrast is found (3.8) and it is noted that for actual targets with a three-dimensional configuration, the polarization degree may be insufficient for detection. The proposed imaging device makes it possible to record not only the degree but also the azimuth of polarization of individual target elements which, in principle, makes it possible to reconstruct the three-dimensional geometrical structure of targets and facilitate their recognition. References 5.

Spectrograph Based on Nonclassical Concave Diffraction Grating With Photodetector Array

937F0077L St. Petersburg OPTICHESKIY ZHURNAL in Russian No 3, Mar 92 pp 41-43

[Article by Ye.A. Sokolova, National Scientific Center at the State Optics Institute imeni S.I. Vavilov; UDC 681.785.552]

[Abstract] The emergence of such new radiation detectors and photodiode arrays and CCD matrices facilitated the development of compact spectrometers. The specific features of developing a video fluorimeter consisting of an excitation polychromator for producing a two-dimensional spectrum at the output and a cell with the substance under study installed in the focusing plane which itself serves as an entrance slit of the recording spectrograph which focuses the spectrum upon the radiation detector array are considered and it is noted that conventional holographic diffraction gratings are not suitable while first-order astigmatism must be corrected. The requirements imposed on the diffraction grating used for this purpose—a nontraditional concave grating—are formulated and the optical train design procedure is outlined in detail. The dependence of the spread function half-width on the entrance slit center height for a spectrograph with and without an illuminator and the dependence of the spectrometer spread function half-width on the wavelength for mirror illuminators with various radii of curvature which correspond to different angles of incidence are plotted. The best image quality is attained with the use of spectrographs with a regular illuminator with a 300 mm^{-1} diffraction grating and a 200 mm radius of curvature or a mirror illuminator with a 75-100 mm radius of curvature. Figures 3; references 15: 13 Russian, 2 Western.

On Controlling Vacuum Deposition of Films

937F0077M St. Petersburg OPTICHESKIY ZHURNAL in Russian No 3, Mar 92 pp 44-45

[Article by V.V. Levdanskiy, V.G. Leytsina, Heat and Mass Transfer Institute imeni A.V. Lykov at the Belarussian Academy of Sciences, Minsk; UDC 539.234]

[Abstract] Extensive uses of chemical vapor deposition for making coats on optical devices are discussed and the possibility of controlling the process of vapor deposition in a vacuum which, unlike the traditional methods, does not call for mutual movement of the source of deposited particles and the substrate or changing the system configuration is examined. In particular, an attempt is made to control the thickness of the film deposited at a given temperature distribution in the channel length with a sublimating internal surface, thus applying the film-forming materials heated to a temperature lower than the melting point and realizing the sublimation phenomenon. To this end, the gas outflow into a vacuum from a cylindrical channel with evaporation (sublimation) and condensation processes occurring on its walls is considered in detail. A geometrical formulation of the problem is plotted and a formula is derived for calculating the relative film thickness, i.e., its thickness divided by its value at a zero cone angle of deposition. The dependence of the relative film thickness on the deposition angle at various relative temperature differentials is summarized. An analysis shows that by manipulating the temperature along the channel, one can produce condensed layers with a sharp decrease in thickness with an increase in the deposition angle as well as films with a sufficiently uniform thickness within a certain angle range. Figures 1; tables 1; references 6: 3 Russian, 3 Western.

Development of Unified Series of Light Microscopes

937F0077N St. Petersburg OPTICHESKIY ZHURNAL in Russian No 3, Mar 92 pp 46-49

[Article by V.P. Balabanovich, T.A. Ivanova (deceased), M.I. Kolpakov, G.I. Maslova, O.N. Nemkova, R.M. Raguzin, A.I. Frez, Leningrad Optics-Mechanics Association imeni V.I. Lenin, St. Petersburg; UDC 681.723]

[Abstract] The history of the development of the first and second generations of aggregate modular light microscopes of the unified MIKRAM series (MICRoscopes, Aggregate Models) is reviewed and the parametric series (PR) of existing microscopes are summarized: transmitted light, transmitted and reflected (incident) light, and analytical microscopes. The theoretical base for the development of the MIKRAM unified series is the systemic approach to group design whereby each device, parametric series, and whole systems are treated as integral systems organized in accordance with an efficiency function and formed from components (SCh) unified by a common goal; and all structures, specifications, development sequence, and other factors and properties are subject to a certain hierarchy. The dependence of the cost of production on the annual production volume, i.e., the economy of scale, is plotted, a block diagram of the unified microscope series, and a block diagram of the component configuration are cited. The concept of parametric series adaptation to the unified series requirements is introduced and it is shown that under today's conditions of the rising demand for microscope and the emergence of new generations of devices, a transition to a unified series creates real opportunities for increasing the design efficiency. It is noted that the development experience of a batch of training and working microscopes which are a part of the MIKRAM unified series will be covered in the next article. Figures 3; references 12.

On Methods of Eliminating Effect of Goniometers' Optical Train Violations on Their Accuracy

937F0077O St. Petersburg OPTICHESKIY ZHURNAL in Russian No 3, Mar 92 pp 53-56

[Article by M.P. Kolosov, Geofizika Scientific Production Association, Moscow; UDC 681.786.3]

[Abstract] Optoelectronic high-precision goniometers with a moving sighting line whose angular displacement is ensured either by theodolites by turning the aiming device or due to the operation of a scanning system are considered. In so doing, attention is focused on new designs which make it possible to construct goniometers in such a way that violation of their optical train during operation does not affect the measurement accuracy. In particular, the specific methods of eliminating the effect of frustrated geometrical design on the goniometer accuracy are addressed and the totality of problems involved in the frustrated goniometer geometry is graphically summarized in the form of a block diagram. Depending on the extent to which the frustrated geometry sources affect the goniometer, two principal cases are examined: the optical elements largely maintain their geometrical similarity; and the optical elements do not preserve their geometrical similarity. Five methods of eliminating the effect of the above factors are investigated and their relative advantages and shortcomings are analyzed. It is noted that only optical methods are capable of producing the angle measurement results in real time under an unstable instrument configuration. Figures 1; references 11.

Method of Comparing Radii of Curvature of Composite Telescope Reflector Elements

937F0077P St. Petersburg OPTICHESKIY ZHURNAL in Russian No 3, Mar 92 pp 57-59

[Article by L.G. Fedina, I.V. Dolik, V.I. Podoba, National Scientific Center at the State Optics Institute imeni S.I. Vavilov; UDC 520.2.062:681.787.7]

[Abstract] The issue of developing multielement sectional astronomical reflectors which have certain advantages over single piece (monolithic) reflectors and the difficulties of fabricating such composite telescope reflectors are addressed; attention is focused on the stringent requirement of ensuring the equality of the elements' radii of curvature, e.g., with a 20 μm tolerance. It is noted that the error of the methods used today is at least 0.01% which does not correspond to the above tolerance for a composite reflector with a 10,000 radius of curvature made from seven 1,000 mm elements. This prompted the development of a method of monitoring the curvature radius which does not call for measuring the absolute values of all elements' radii of curvature. To this end, a relative monitoring method was developed on the basis of a white light interferometer installed at the center of curvature of the reflector under study whereby the latter is compared to a standard reflector with a certified radius of curvature. The essence of the method is considered using the example of an interferometer with a scattering plate (IRP). The optical design of the comparator is cited and the interference patterns of phase reflectors obtained in white light are plotted. The accuracy of the method is assessed by analyzing the errors affecting the surface shape monitoring results. An experimental check of the method was performed using 150 and 90 mm dia. reflectors with a 1,032.8 mm radius of curvature. The experiments fully confirmed the possibility of comparing radii of curvature accurately within tens of micrometers; the method is recommended for use in composite reflector element production. Figures 4; references 8: 5 Russian, 3 Western.

Method of Determining Wavelength of Spectral Lines Recorded by Multielement Photodetector

937F0077Q St. Petersburg OPTICHESKIY ZHURNAL in Russian No 3, Mar 92 pp 60-63

[Article by A.P. Demin, F.F. Sultanbekov, O.B. Yandueganova, State Applied Optics Institute, Kazan; UDC 681.785.5:621.383]

[Abstract] The lack of detailed data on spectral line identification in multielement photodetectors prompted the development of methods of determining the wavelength of the spectral lines recorded by such multielement detectors and increasing the identification accuracy. A specific method of equating the spectral line position with the photodetector element number with the maximum signal is addressed and it is speculated that the spectral line wavelength measurement accuracy can be increased significantly by using the coordinate of the line image center of gravity as the intensity maximum coordinate of the spectral line. A formula is derived for refining the positions of the intensity maxima of the reference and target spectral lines; the spectral line outline is approximated by s symmetric step function and it is assumed that the spectrometer spread function is symmetric. Other methods of approximating the spectral line outline are considered. Several methods of determining the spectral line position are summarized at a 3,650.15 and 3,663.28 angstrom wavelength; an analysis shows that the best results are attained using the method described in USSR patent No. 1603202 (*Byulleten izobreteniy* No. 40, 1990, p. 170). It is noted that attempts to improve the spectral line wavelength measurement accuracy were unsuccessful due to the fact that a photodetector whose element width is not optimal for reconstructing the spectral line outline was used. Figures 2; tables 1; references 9: 6 Russian, 3 Western.

Small Temperature-Controlled Cryostats for Optical Research

937F0077R St. Petersburg OPTICHESKIY ZHURNAL in Russian No 3, Mar 92 pp 64-68

[Article by A.G. Demishev, D.P. Pelykh, A.K. Shirkov, S.A. Uksusova, S.I. Dubinskiy, Donetsk Engineering Physics Institute; UDC 536.581.3:535]

[Abstract] The advantages of small continuous flow cryostats which can be refilled from a mobile Dewar flask and the increasing use of various cryogenic attachments to commercial spectrophotometers and dedicated comprehensive systems prompted a study of the design and characteristic features of temperature-controlled cryostats for studying the optical properties of samples in a vacuum. The effect of the quality of vacuum (ensuring the sample surface purity) on the confidence of results and the need to develop a good vacuum are discussed and two ways of solving this problem are considered; attention is focused on installing a built-in cryogenic pump and developing a special type of sample holder. The dependence of the holder temperature on the liquid nitrogen rate in two cryostat series—KP and KPO—under various conditions are plotted and it is shown that both series ensure prompt experiment preparation and execution and high confidence of the results. The small size and weight of the cryostats make them suitable for use as a cryogenic attachment to most spectrometers while detachable windows make it possible to examine samples in any band. The operating temperature is controlled within 3-300K by pumping the cryogenic agent. In most cases, a temperature stability on the order of 0.05K is ensured under 80K and on the order of 0.5K under 300K. Figures 4; references 18: 11 Russian, 7 Western.

Use of Photoelectric CCD Analyzer in Monitoring Submicrometer Linear Objects

937F0077S St. Petersburg OPTICHESKIY ZHURNAL in Russian No 3, Mar 92 pp 68-71

[Article by S.O. Yezerskiy, G.A. Syrevich, V.V. Kalashnikov, Kiev Branch of the Scientific Research Institute of Optical Instrument Engineering; UDC 621.383.72+681.723]

[Abstract] The increasing need for computer-aided monitoring and measurement of the planar orientation of linear objects with submicrometer dimensions and the trend toward decreasing the magnetic head clearance prompted an investigation into the possibility of increasing the accuracy characteristics of the instruments used to monitor the orientation of blanks by the image of the clearance whose dimensions in the object plane is between 0.3 and 0.7 μm. To this end, a photoelectric analyzer on the basis of an FPPZ-2L (or FPZL-1L) linear CCD (PZS) installed in the optical microscope image plane is used. The timing charts of the signal preprocessing device (i.e., video processor) operation are plotted. An analysis of the oscillograms of the image signal at the CCD output shows that due to the low image contrast, the signal:noise ratio is also low; the factors affecting this ratio are summarized. The operating principles of the CCD-based analyzer are described in detail and the device is recommended for use in a unit for oriented video head cutting together with the optical channel for preliminary visual positioning and alignment. A blank positioning accuracy of 2 min (of angle) is attained. The 50 dB SNR attained in the device calls for further studies aimed at measuring the width of objects with a 0.03 μm minimum dimension by the image reconstruction method. Figures 2; references 5.

Geometrical Correlations of Method of Measuring Transparent Cylindrical Object Parameters Using Scattered Light

937F0091A Moscow METROLOGIYA in Russian No 3, Mar 92 pp 21-26

[Article by V.F. Grishko, S.D. Khomuk; UDC 681.786]

[Abstract] The lack of mass produced facilities for measuring the inside diameters of pipes and refractive indices of transparent cylindrical objects (PTsO)—capillaries, optical fibers, etc.—by irradiating the objects with collimated wide or narrow light beams necessitated the development of new methods of measuring these parameters; attention is focused on using scattered light for deriving information about cylindrical transparent objects. The method amounts to irradiating the objects with scattered light, bounding a part of scattered light with opaque screens, shaping parallel rays transmitted through the object with the help of an objective lens, and projecting the beam parallel to the measurement axis upon the sensitive layer of a photodetector. A schematic diagram of the method is cited and formulae which connect the outer boundaries of light and shadow with the limiting entrance angle of rays at the object are derived. A comparative computer analysis of traditional methods and the new technique shows that the error components due to the object motion in space can be decreased by an order of magnitude in the latter case. The scattered light method is characterized by a broad range of measured values and can be used in such areas as measurements of graded index optical fibers and liquid media and detecting bubbles in fiber blanks. Figures 1; references 5: 4 Russian, 1 Western.

Optical Soliton Amplification. Adiabatic Approximation

937F0085A St. Petersburg OPTIKA I SPEKTROSKOPIYA in Russian Vol 72 No 5, May 92 pp 1145-1151

[Article by A.I. Maymistov, Moscow Engineering Physics Institute; UDC 535.2]

[Abstract] Amplification of optical solitons used to convey information in fiber optic communication lines, particularly coherent propagation of ultrashort pulses (UKI), is considered in the framework of a two-level atom model. Group velocity variance is taken into account on the lowest order while the nonlinear susceptibility variance of the material from which the single-mode fiber is made is ignored. The theoretical analysis is based on the adiabatic approximation which has been used successfully for solitons in the perturbation theory. The principal equations of the model describing the

ultrashort pulse's electric field envelope behavior and the state of impurity atoms in the fiber are derived and the adiabatic approximation of the nonlinear Schroedinger equation (NUSh) is formulated. An analysis of the adiabatic approximation is performed for a wide nonuniformly broadened line with a Lorenz shape and the law of the ultrashort pulse amplitude change along the exclusive phase plane line, i.e. the amplified soliton without initial phase modulation, is derived. The limiting values of the amplitude soliton for the broad and broadened narrow lines differ by the dependence of the amplitude on the fiber length, i.e., gain increments. The conclusion is drawn that during the amplification, the UKI amplitude increases monotonically and its duration decreases and approaches the limiting value. The adiabatic approximation's shortcoming is the fact that it totally ignores the ultrashort pulse disturbances appearing on its trailing edge in the form of envelope oscillations. The need to study this phenomenon further is stressed. References 20: 5 Russian, 15 Western.

Multiple Nutation Echo Structure Under Excitation Conditions of Nonuniformly Broadened Optical Line by Doubled Light Pulse

937F0085B St. Petersburg OPTIKA I SPEKTROSKOPIYA in Russian Vol 72 No 5, May 92 pp 1152-1161

[Article by V.S. Kuzmin, Solid State and Semiconductor Physics Institute, Minsk; UDC 535.2]

[Abstract] Single-pulse echo and multiple double-pulse echo structure generation under the effect of nonresonant pulsed excitation of a two-level atomic system and a similar problem for coherent phenomena appearing during the action of the pulse, i.e., the nutation effects, are discussed and an attempt is made to demonstrate that in addition to a trivial decrease in the nutation amplitude, the nonresonant excitation nature leads to the appearance of multiple echo signals whose formation time and amplitude depend on the correlation of the Rabi frequency, the off-resonance detuning, and nonuniform line width. The problem is considered using the example of nutations in a two-level atomic system excited by a doubled light beam—a superposition of two rectangular pulses of the same frequency but with different amplitudes. The amplitude variation law formula and an expression for the polarization components are derived. The feasible domain of the nutation response as a function of the doubled pulse parameters is determined and the nutation response behavior after the action of the doubled pulse is plotted. Optimum nonresonant echo signal observation conditions are discussed and it is noted that the coherent response evolution can be interpreted as an oscillation process. The findings confirm the possibility of observing multiple nutation echo signals which are due to zero beats of the polarization oscillations at variable frequencies and the generalized Rabi frequency. The author is grateful to L.N. Makutin for computer processing of analytical expressions. Figures 4; tables 1; references 8: 5 Russian, 3 Western.

Optical Data Processing When Phase Memory Is Available

937F0085C St. Petersburg OPTIKA I SPEKTROSKOPIYA in Russian Vol 72 No 5, May 92 pp 1162-1165

[Article by L.A. Nefedyev, Kazan State University; UDC 535.2+535.317.1]

[Abstract] Echo holography applications for signal filtering in optical data processing systems and other areas and echo hologram recording in gaseous media where more efficient processing of stored data is possible are discussed and the theory of echo hologram formation in the case where the reference or reading pulse has a specified space-time structure, i.e., develops spatial frequency selectivity of the gaseous medium, is developed. An attempt is made to demonstrate that in the case of a pure phase object, one can select the reference filtering pulse which transforms phase data on the object into an amplitude information. The process of echo hologram formation in a gas by stimulated photon echo and the issue of phase contrast in echo holography are considered in detail. It is shown that in the case where the first and third of the three pulses have a frequency spectrum overlapping with the spectral width of the resonant transition, the object field can be simply reproduced in the echo hologram response but the reference and reading pulses must have specified phase characteristics. Due to the possibility of transforming phase data into amplitude data on the object, echo holography is an analogue of phase contrast in optics. The only principal difference is the fact that in the case with echo holograms, the phase-to-amplitude information conversion is performed by the resonant gaseous medium itself which does not contribute additional distortions. References 16: 13 Russian, 3 Western.

Multiple Scattering Effects in Laser Diagnostics of Biological Objects

937F0085D St. Petersburg OPTIKA I SPEKTROSKOPIYA in Russian Vol 72 No 5, May 92 pp 1171-1177

[Article by I.L. Maksimova, S.N. Tatarintsev, L.P. Shubochkin, Saratov Branch of the Radio Engineering and Electronics Institute of Russia's Academy of Sciences; UDC 535.36+621.373:535.06]

[Abstract] Interest in radiation propagation in disperse media with a high scattering center concentration, such as biological tissue and biological suspensions, where reradiation among particles may affect the measurement results prompted an examination of the theory of multiple scattering based on Mie's solution for single light scattering by a single spherical particle which is transformed in order to derive an expression for the light scattering intensity directly through the scattering particle parameters, without first computing the amplitudes. The scattering intensity of nonpolarized light is represented in the form of a Legendre polynomial series; the electromagnetic wave propagation and scattering in a random cloud of scatterers is described with the help of an integral transport equation. Incidence of a planar wave normal to the surface of a flat layer

containing randomly arranged particles is considered and matrix notation is used to describe the effect of multiple scattering on the polarization characteristics. The indicatrix of diffusion of an infinite planar wave on the flat layer of spherical particles of polystyrene latex and its first and second approximations, the angular dependence of the proportion of doubly scattered radiation relative to the total scattered radiation flux, and the intensity distribution diagram of light with various scattering ratios as a function of the optical layer depth are plotted. The effect of multiple scattering on the elements of the light scattering matrix (MRS) by disperse media and their attenuation is analyzed. The study of the effect of reradiation on the angular distribution of light scattering in disperse media makes it possible to explain some characteristics of experimental light scattering matrices and assess the contribution of multiple scattering to the recorded intensity. Figures 4; references 5: 3 Russian, 2 Western.

On Possibility of Transmission Hologram Recording in Denisyuk Design

937F0085E St. Petersburg OPTIKA I SPEKTROSKOPIYA in Russian Vol 72 No 5, May 92 pp 1195-1200

[Article by A.P. Yakimovich, Physics Institute imeni P.N. Lebedev, Moscow; UDC 535.317.1]

[Abstract] Two simple methods of recording transmission holograms using Denisyuk's optical design whereby the object of holography is located in direct proximity to the hologram, which considerably relaxes the requirements imposed on the restoring light source and makes it possible to reconstruct or observe the image on both sides of the hologram, are considered. In recording the hologram, a semireflecting mirror (PZ) and the object are placed on different sides of the photographic material (G), so a proportion of the reference wave transmitted by the semireflecting mirror and the photographic material illuminates the object while the signal wave transmitted by the photographic material is partially reflected by the mirror and creates the second signal wave which corresponds to the reflected object image in the mirror. After the interference pattern is recorded, three partial subholograms are formed in the photographic medium. During the image reconstruction, the signal wave is restored and diffracted on the reflecting transmitting subhologram, and restores the reference wave. The hologram's diffraction efficiency is assessed. It is noted that the two methods are especially promising for making circular scanning holograms since they make it possible to bring the photographic material flush with the object and develop a compact hologram with a wide angle of view in the vertical direction. Figures 2; references 3: 2 Russian, 1 Western.

On Characteristics of Recording Relief Hologram Structures on Thin Layers of PE-2 Photoemulsion Using Pulse Laser

937F0085F St. Petersburg OPTIKA I SPEKTROSKOPIYA in Russian Vol 72 No 5, May 92 pp 1201-1205

[Article by S.N. Koreshev, T.Ya. Kalnitskaya, B.S. Guba, State Optics Institute imeni S.I. Vavilov, St. Petersburg; UDC 535.317.1]

[Abstract] The conditions for recording holographic optical elements (GOE) are discussed and it is noted that known techniques do not make it possible mechanically to transfer the holographic optical element recording procedure developed for CW lasers to pulse lasers. The peculiar features of using thin (less than 1 μm) photoemulsion layers for recording phase relief holographic structures with the help of the second harmonic emission of a Nd-glass laser with a 50 ns pulse duration and an exposing laser radiation wavelength of 0.53 μm are examined using layers of the PE-2 photoemulsion sensitized by a 1241 spectral sensitizer for the green spectrum range. The silver halide layers are applied to a glass base by centrifuging. The tests include monopulse interference pattern recording, monopulse recording with subsequent exposure to one, two, and more pulses from the same laser while covering one recording interferometer arm, and monopulse recording with subsequent exposure to a CW laser at a 0.515 μm. An analysis shows that monopulse recording without subsequent exposure cannot be used for making relief holograms; this is attributed to violations of the interchangeability law. A comparison of the relief depth of the holographic structures with additional exposures shows that additional exposure by the pulse laser radiation ensures the greatest relief depth. The dependence of the relief depth on exposure is plotted. Successful recording of a 0.2 μm deep relief in a 0.4 μm-thick layer with a photoemulsion speed of 0.1-0.2 mJ/cm^2 with additional pulse laser exposure points toward a good outlook for using these photolayers for GOE recording with the help of pulsed nanosecond lasers. The authors are grateful to V.K. Elts, M.A. Gavrilova, and O.P. Zhuk for help with the experiments. Figures 3; references 11: 10 Russian, 1 Western.

Conical Radiation and Parametric Amplification in Atomic Vapors in Strong Light Field

937F0085G St. Petersburg OPTIKA I SPEKTROSKOPIYA in Russian Vol 72 No 5, May 92 pp 1241-1247

[Article by I.S. Zeylikovich, Grodno State University; UDC 535.2:539.18]

[Abstract] The inconsistency of existing theories of conical radiation and attempts to attribute to the four-wave parametric interaction (ChPV) as well as the abnormally high conical radiation gain and its threshold character prompted a study of the quantitative characteristics of conical radiation in atomic vapors and an attempt to interpret it as radiation in the direction of phase matching of composite waves and degenerate Stokes and anti-Stokes radiation under threshold parametric amplification during interaction with the pump wave. The experiment reveals that conical radiation is amplified sharply when the maximum of its Stokes wing falls outside the absorption line contour. The study shows for the first time that conical radiation has two thresholds determined by the pump wave intensity: when the first threshold is reached, spontaneous emission of independent atoms turns into conical radiation (KI) in the direction of phase synchronism and when the second is

reached, the above parametric amplification jump occurs due to a sharp decrease in absorption. References 8: 3 Russian, 5 Western.

Investigation of Sharpness Function Properties of Noncoherent Images of Extended Objects

937F0085H St. Petersburg OPTIKA I SPEKTROSKOPIYA in Russian Vol 72 No 5, May 92 pp 1260-1266

[Article by G.N. Maltsev, A.G. Lobanov, Military Engineering Academy imeni A.F. Mozhayskiy, St. Petersburg; UDC 535.317.1]

[Abstract] Traditional functions of sharpness of high-resolution optical data processing systems employing adaptive optical signal correction, i.e., functionals of the field strength distribution in the image plane, are outlined and the difficulties of monitoring extended objects in the absence of a reference point source due to phase distortions are noted. New spectral sharpness functions are suggested and the effect of the correlation between the uncertainty domain and the monitored object contour, i.e., the accuracy of the contour estimate, as well as the background noise through which the image is formed on the traditional and proposed spectral sharpness functions is examined. The noncoherent image realization of a rectangular test object under various phase distortions and the dependence of the sharpness function on the RMS values of simulated phase distortions are plotted. These curves are equivalent to the adaptive circuit's discrimination characteristics and demonstrate that traditional sharpness functions are efficient only if the monitored object's contour is precisely known and the background noise level is low. Spectral sharpness functions, on the other hand, are suitable for extended objects of unknown shape since the discrimination curve shape does not depend on the noise level and *a priori* shape estimate accuracy. The need for special studies of coherent images is stressed. Figures 3; references 14.

Precise Formula for Analyzing Ray Path Through Spherical Geodesic Lens

937F0085I St. Petersburg OPTIKA I SPEKTROSKOPIYA in Russian Vol 72 No 5, May 92 pp 1267-1272

[Article by A.P. Smirnov, State Optics Institute imeni S.I. Vavilov, St. Petersburg; UDC 535.3]

[Abstract] The uses of geodesic lenses for focusing and collimating radiation and the difficulty of the ray path analysis task are discussed and a ray path analysis formula which is free of these shortcomings is derived. To this end, the function describing the geodesic line on a torus is expanded into a Taylor series and its accuracy is compared to that of V.E. Wood's formula. The comparison shows that the quadratic approximation of the proposed formula has a smaller systematic error (by up to 15-20 times) and a less pronounced dependence of the calculation error on the angle of incidence than Wood's formula. The study shows that in analyzing the ray path, it is necessary to take into account the following parameter ranges: the ray incidence height and the smoothing edge radius. This makes it possible to determine the power of the expansion polynomial which ensures the required calculation accuracy. Figures 3; references 5: 2 Russian, 3 Western.

Effect of Anisotropy of Films With Nonlinear Parameters on Self-Induced Transparency Phenomenon in Optical Waveguide Structures

937F0085J St. Petersburg OPTIKA I SPEKTROSKOPIYA in Russian Vol 72 No 5, May 92 pp 1273-1276

[Article by A.G. Glushchenko, Radio Engineering and Electronics Institute of Russia's Academy of Sciences, Fryazino; UDC 621.372.8:535]

[Abstract] The role of transition layers and interface films, especially films with nonlinear polarization, in forming wave processes is discussed and the lack of data on the effect of anisotropy on the physical properties of bounded media is noted. The effect of the anisotropy axis orientation in a film with nonlinear parameters on the properties of a planar waveguide made as a system of three isotropic magnetodielectrics with linear parameters and a film with nonlinear parameters on one of the interfaces characterized by a certain component of the nonlinear polarization vector is considered. The wave equations are solved. An analysis of the formulae shows that a change in the anisotropy axis orientation in the nonlinear part of the polarization vector makes it possible to control the parameters of the solitons forming there and may lead to an instability of their parameters and create bound states of the *E*- and *H*-solitons; this factor must be taken into account in studying the parameters of films or designing functional elements on their basis. Figures 1; references 4.

Excess Optical Radiation Attenuation in Optical Waveguides in Optical Cables

937F0085K St. Petersburg OPTIKA I SPEKTROSKOPIYA in Russian Vol 72 No 5, May 92 pp 1277-1282

[Article by S.I. Ivlev, V.B. Smirnov, St. Petersburg State University; UDC 666.189.2:535]

[Abstract] The structure of optical cable is summarized and it is shown that usually, the optical fiber (VS) has a primary protective cladding applied during its pulling or in a subsequent coating operation—the primary optical module. This module is often encased in a polymer tube which is referred to as the secondary optical module which may contain several primary modules. The optical cable (OK), in turn, may contain several secondary modules. The optical radiation attenuation in optical

fibers at various stages of actual optical cable manufacturing and in its final form is examined due to the fact that attenuation in cables often increases significantly under the effect of temperature drops, shock, vibrations, hydrostatic pressure, cyclical winding and rewinding, and tensile forces. The behavior of attenuation at successive optical cable manufacturing stages, the protective module tube shrinkage, the back scattered signal curves in optical fibers with an alternating-sign spiral (ZPS) shape, and the bar chart of the optical fiber excess distribution in an actual cable are plotted. The protective tube shrinkage may reach 1.5% thus leading to excess fiber lengths. An analysis shows that the alternating-sign spiral shape which the fiber assumes in the cable is the primary cause of excess attenuation. Typical materials used for making commercial optical cables are surveyed. Figures 4; references 7: 4 Russian, 3 Western.

On Role of Alternating-Sign Spiral in Optical Radiation Attenuation Increment in Optical Fibers of Optical Cables

937F0085L St. Petersburg OPTIKA I SPEKTROSKOPIYA in Russian Vol 72 No 5, May 92 pp 1283-1288

[Article by S.I. Ivlev, A.A. Merkulov, V.B. Smirnov, St. Petersburg State University; UDC 666.189.2: 621.371.801]

[Abstract] The effect of the optical fiber excess inside the protective polymer tubes or cavities inside the optical cable due to the difference in the optical fiber and protective element shrinkage under the effect of external conditions on the optical fiber shape—it assumes the form of an alternating-sign spatial spiral (ZPS) whose rotation direction changes due to torsional vibrations—is discussed. Scalar expressions reflecting the optical fiber shape are derived. To check the adequacy of the mathematical model and clarify the fiber parameters, the radii of curvature and lead of the helix as well as the optical loss increment as a function of the excess optical fiber length in the optical cable are determined. The probability of given radii and helix leads for a specified excess, the result of shaking a module with a given excess, and the dependence of attenuation on the optical fiber radius of curvature are plotted. The findings confirm the dominant role of the alternating-sign spiral formation on the increase in attenuation; in particular, the microbends forming in the alternating-sign spatial spiral as a result of the fiber pressure on the module wall have the greatest effect on attenuation. The role of coated optical fiber friction is discussed and the friction coefficients of epoxyacrylate, polyamide, and polyacrylate vs. 40-Sh fluoroplastic, low-pressure polyethylene, and high-pressure polyethylene with and without lubrication are summarized. Figures 4; tables 1; references 5: 4 Russian, 1 Western.

Experimental MHD Unit With Superconducting 'Sever-M' Magnet

937F0071A Moscow DOKLADY AKADEMII NAUK in Russian Vol 326 No 4, 92 pp 642-646

[Article by R.V. Dogadayev, N.P. Kolyadin (deceased), O.G. Matveyenko, V.P. Panchenko, Ye.P. Polulyakh, A.A. Yakushev, Atomic Energy Institute imeni I.V. Kurchatov, Moscow and Troitsk Institute of Innovative Nuclear Fusion Research; UDC 533.99:538.945: 621.362]

[Abstract] An experimental Sever-M MHD (MGD) unit designed and assembled for an experimental verification of the physical and engineering designs of MHD units with superconducting magnetic systems (SMS) operating in the pulsed periodic and recurrent intermittent conditions is described. The unit consists of plasma generators, an MHD channel, a superconducting magnetic system, a load unit, recording instruments, and experiment control devices. The design and operating principle of each component is outlined in detail and the profile of the flow section of the Pamir-1PE MHD channel's gas dynamic section as well as the magnetic field profile of the superconducting model and the electrode zone position relative to the magnetic field profile are cited. Technical data of the full-scale experiment conducted in the Sever-M unit are summarized. The initial segments of the time dependence of the current and voltage on the load in a static magnetic field and with an increase in the plasma generator pressure and the calculated voltage-current characteristics and load characteristics of the MHD generator under various magnetic field induction levels are plotted. A numerical study of the flow and energy characteristics of the MHD generator is conducted with the help of a quasitwo-dimensional model of two-phase polydisperse flow and Kanal-1 software. It is noted that as the magnetic field increases to the limiting value, the electric power of the unit may increase by up to 1.5 times. The conclusion is drawn that the MHD generator with the Sever-M superconducting magnetic system has a reliable design and confirms the possibility of using MHD units with superconducting magnetic systems in the pulsed periodic and recurrent intermittent conditions. When operating with combustion products of solid plasma fuel at a magnetic induction of 3 T and electric power of 5.4 MW, the unit develops a specific energy efficiency of 0.33 MJ/kg and a power density of 350 MW/m^3 with a settling time of 0.1 s. Figures 4; tables 2; references 3: 1 Russian, 2 Western.

Structure of Multichannel Interference Measuring Systems for Precision Inspection of Objects' Geometric Characteristics

937F0082A Leningrad IZVESTIYA VYSSHIKH UCHEBNYKH ZAVEDENIY: PRIBOROSTROYENIYE in Russian No 9, Sep 92 (manuscript received 20 Dec 90) pp 59-66

[Article by I.P. Gurov and I.M. Nagibina, Leningrad Institute of Precision Mechanics and Optics; UDC 531.715.1.089.68]

[Abstract] A systems approach has been proposed that makes it possible to select the optimal structure and functional criteria for an interference multichannel measuring system for precision inspection of objects' geometric characteristics. According to the scheme proposed, each of a measuring system's channels may be classified as either a basic or auxiliary channel. Basic channels are further classified as spectral, polarization, spatially separated, time, and power channels. Auxiliary channels may be either optical or photoelectric channels. Their main purpose is to reduce the effect of variations in the parameters characterizing the measuring system's environment and as such are subclassified as power, refractometric, thermometric, barometric, and humidity-measuring channels. Parallel, spatially separated measuring channels, including those operating within the confines of a common interference field, are given special attention. Spectral selection based on wavelength at interferometers' outputs is said to be rarely used, whereas methods of spectral separation of the components of photoelectric signals in modulation and heterodyne interference systems are widely used. Interference devices containing optical channels with polarization separation and a two-beam circuit are also widely popular. The advantage of polarization circuits is that they offer the possibility of geometric combination of the interferometer's branches with subsequent polarization separation of the paths of the reference and measuring waves' propagation, thus providing insensitivity to the effect of the instability of the characteristics of an interferometer's individual components. Measuring channels with time separation may be established in both the optical and photoelectric parts of a measuring system. Phase-shift interferometers produce a set of interference patterns with a mutual shift with respect to the magnitude of phase difference at individual points in time, whereas photoelectric channels with time separation are based on the principle of strobing and switching interference signals. Measuring channels separated on the basis of a power criterion are based on the method of amplitude selection of the values of the interference signal by using multichannel photoelectric recording. Auxiliary photoelectric channels of this type are used to stabilize a radiation source's power. When measuring systems containing several types of measuring channels they are termed combined measuring systems. Recognition of the common design and structural features shared by different types of measuring systems makes it possible to analyze their characteristics on the common ground of the theory of multidimensional signals and systems. Figures 4; references 7: 6 Russian, 1 Western.

Special Television System

937F0082C Leningrad IZVESTIYA VYSSHIKH UCHEBNYKH ZAVEDENIY: PRIBOROSTROYENIYE in Russian No 9, Sep 92 (manuscript received 25 Jan 91) pp 76-80

[Article by B.V. Zakharov (deceased) and B.A. Kruming, Tallinn; UDC 621.397]

[Abstract] When studying optically heterogeneous media by means of optical radiation (coherent optical radiation in particular), researchers must address the problem of analyzing the dynamics of the effect of the heterogeneities on this radiation. This effect may include one or more of the following: diffraction, interference, scattering, and self-focusing. Television systems based on linear and matrix photosensitive instruments with charge transfer may be used for such purposes. By using coherent optical radiation, one may create a stationary spatiotemporal radiation field structure whose parameters (power, carrier frequency, phase shifts, etc.) remain constant throughout the course of given measurements. A special television system has been developed to measure the heterogeneities of optically transparent media placed in the interference field of a coherent source. The magnitude of heterogeneities may be identified and measured from the degree of bending of the interference bands as the information pattern is projected onto a photoreceiver with charge transfer. The television system operates in an electronic shutter mode. The position of zones of uneven illumination is recorded in two stages involving 1) the recording of video signals (that have been converted into digital form) into memory after one-time scanning of a line of photosensitive elements and 2) a series of comparisons that ultimately result in the output of the relative time coordinates specifying the positions of the said zones. The distinction of the new use lies in the fact that the signals from its first output enter the control inputs only after the appearance of a signal from the charge-coupled device from the first photosensitive element. The new television system makes it possible to analyze an optical image in a dynamic mode with a more than 100-fold increase in the precision of determining the specified information parameter as compared with the capability of television structures based on a linear photoreceiver with charge transfer. Figures 2; reference 1 (Russian).

A Model of the Opticoelectronic Image of a Relief Scene

937F0082D Leningrad IZVESTIYA VYSSHIKH UCHEBNYKH ZAVEDENIY: PRIBOROSTROYENIYE in Russian No 9, Sep 92 (manuscript received 18 Feb 91) pp 83-87

[Article by S.N. Samoylov, Kharkov Electronics Institute; UDC 621.383.8:621.3]

[Abstract] The literature includes models of machine vision involving misfocusing that is constant throughout the plane of the image and isotropically radiating points of the specimen. Such models correspond to systems with a relatively low resolution. The model proposed herein gives consideration to variable misfocusing caused by the relief and to anisotropy of the radiation of the points of a scene. The proposed model makes it possible to use a computer to develop a numerical representation of the signals at the output of an image input device. The mathematical model presented includes functions modeling the relief of the scene (the function h), the radiation of the scene, and the optical image on the plane of the photoelectric converter. The conversion of the optical image into electrical signals

by a linear system is modeled in terms of a superimposition integral. A discrete representation of the model is proposed. An expression for interpolating the function *h* is also provided. The estimating expression provides an acceptable degree of accuracy and makes it possible to avoid the deadlock that may arise in cases where *h* changes so quickly that the newly found nodes coincide with the preceding nodes. Figure 1; references 4 (Russian).

Model of the Microprocessor Direction-Finding Channel of a Laser Detection and Ranging System

937F0082E Leningrad IZVESTIYA VYSSHIKH UCHEBNYKH ZAVEDENIY: PRIBOROSTROYENIYE in Russian No 9, Sep 92 (manuscript received 14 Feb 91) pp 87-91

[Article by I.A. Lapshina, Leningrad Institute of Precision Mechanics and Optics; UDC 681.42.39]

[Abstract] A microcomputer operating algorithm is proposed for use in estimating the azimuth and tilt angle in laser detection and ranging systems. In essence, upon receiving data establishing the amplitude of the laser detection and ranging system's sounding pulse reflected from the target, the angular position of the scanner's axis, and the distance to the target with an interval equal to the sounding pulses' repetition period, the microcomputer issues an estimate of the target's deviation with respect to tilt angle and azimuth. A mathematical model of a microprocessor estimator of tilt angle and azimuth in terms of a linear nonstationary digital filter is presented. The model presented makes it possible to study the dynamic properties of a microprocessor estimator on precision of estimation, as well as to give consideration to the dynamic properties of the estimator when synthesizing control algorithms in systems for tracking a target based on angular coordinates. Figures 3; references 3 (Russian).

A Study of the Effect of Preloading on the Elastic Characteristics of Slotted Springs

937F0082F Leningrad IZVESTIYA VYSSHIKH UCHEBNYKH ZAVEDENIY: PRIBOROSTROYENIYE in Russian No 9, Sep 92 (manuscript received 30 Nov 90) pp 46-50

[Article by V.Ye. Sidorov, Ufa Aviation Institute imeni Sergo Ordzhonikidze; UDC 62-272]

[Abstract] Slotted springs are widely used in instrument making as elastic supports and guides. A study was conducted to find ways of preloading slotted springs so as to improve the elastic characteristics of scragged slotted springs (i.e., reduce their nonlinearity and thereby reduce their loss of stiffness when in a flat state when the amount of scragging (the distance between a spring's rings along its axis) is increased. The studies performed established that the elastic characteristics of a slotted spring depend not only on its geometric parameters but also on additional force factors between the spring's rays (i.e., the deformable elements connecting the spring's rings) created by preloading. A slotted spring with rays having the following geometric dimensions was used in the studies: average radius, 15.9 mm; width, 1.25 mm; thickness, 0.12 mm; central angle, 1.9 radians; and amount of scragging, 4.8 mm. Several preloading techniques were used, including methods involving shifting the ring sectors in their plane relative to their position in an identical slotted spring but without separating the rings. Force factors acting on the ends of the rays in the plane of the rings were found to have the greatest effect on a slotted spring's stiffness. By controlling the amount of intermediate scragging, the researchers were able to regulate the stiffness of a slotted spring from a value approximately equal to the stiffness of a flat slotted spring to zero. Surprisingly, however, the magnitude of a slotted spring's supporting force when in a flat state was found to be virtually independent of the amount of intermediate scragging. Figures 4; references 3 (Russian).

Estimating the Duration of Automated Tests of Opticoelectronic Instruments

937F0082B Leningrad IZVESTIYA VYSSHIKH UCHEBNYKH ZAVEDENIY: PRIBOROSTROYENIYE in Russian No 9, Sep 92 (manuscript received 7 Mar 91) pp 66-71

[Article by Ye.Yu. Merzlyutin, Leningrad; UDC 621.383.8]

[Abstract] Modern opticoelectronic instruments are used for many different purposes and may thus be placed on a variety of different carriers or else used in ground systems at test ranges. In recent years, the amount of information processed by such instruments and the number of information streams output by them have increased by two to three orders of magnitude. The increased capabilities of opticoelectronic instruments and the increased requirements imposed on them (e.g., regarding accuracy and stability) have meant that durations of the automated tests to which such instruments are subjected prior to use have become impracticable (they are often comparable to the instrument's total useful life). The problem of estimating the time required for adequate automated testing of opticoelectronic instruments with multicomponent photoreceivers is examined. Mathematical formulas for estimating test duration are presented along with recommendations regarding reducing test duration. The formulas presented give consideration for such factors as the test stand's degree of automation, the optimality of the computer equipment used, and the efficiency of the testing algorithms and software used in the testing. The recommendations regarding minimizing the test duration center around the principle of grouping the results of individual measurements by the type of bench equipment used and by the type of opticoelectronic instrument parameter or characteristic being determined and then optimizing the testing procedures used on each of the identified groups. Emphasis is placed on reducing the time required to prepare measurements and transfer test objects to different parts of an opticoelectronic instrument's field of view and on

increasing the number of photoreceiver elements simultaneously illuminated by test objects. Optimization of testing algorithms and software is recommended as one of the simplest places to begin the process of reducing test duration. References 3 (Russian).

Drifting Buoy in Oyashio Anticyclonic Gyre

937F0057A Moscow DOKLADY AKADEMII NAUK in Russian No 3, 1992 pp 547-550

[Article by K. A. Rogachev, E. Karmak, M. Miyaki, R. Tomson, G. I. Yurasov; presented by academician V. I. Ilichev 29 Apr 92; UDC 551.465]

[Text] 1. In the region of subarctic rotation western boundary currents of the northern portion of the Pacific Ocean—the Oyashio and Kamchatsk—consistency of anticyclic gyres is observed. During good weather conditions, satellite infrared images allow 3-4 such gyres to be identified. These gyres are located along the Kurile-Kamchatka channel from the southern Kurile islands to the southern tip of the Kamchatka peninsula.

The Kuroshio WCR86B warm anticyclonic gyre separated from the first branch of Kuroshio in 1986. Continuous satellite images of the subarctic frontal zone and sequential hydrographic surveying on ships of the Pacific Oceanological Institute and the Far East Regional Institute were used to track the gyre (1-3). In September of 1990 the gyre reached the latitude of the Bussol Straight. Its position in September of 1990 was determined by two independent hydrographic surveys. In October 1990 hydrographic sections again cut across the WCR86B gyre. The age of the WCR86B gyre in 1990 was 4.5 years. Its vertical structure was characterized by a warm nucleus in the upper layer and a nucleus of waters of reduced salinity in the 250-600 meter layer.

2. In May of 1988, the currents in the WCR96B gyre were measured with drifting buoys (1). Seven surface drifters showed that the water rotation period on the periphery of the gyre is 7-8 days. In November 1990 three ARGOS drifters were placed in the central portion of the gyre and along its edges. The buoys had a sock type sail 6 meters long and 1 meter in diameter. The sail was placed at a depth of about 15 meters. The buoy locator satellite system allowed the position of the buoys to be determined 7-8 times per day with an accuracy of about 250 meters.

3. The average speed of drift changed depending upon the azimuthal and radial location of the buoys. All the buoys showed a high amplitude of near-inertial movement. The most complicated trajectory was observed for the buoy which was placed in the central portion of the gyre (fig. 1). Within 40 days the buoy made five complete revolutions with an increasing radius of turn. In 1990 the average period of turn of the buoy in the gyre was also about 7 days. The pronounced high frequency oscillations were observed when the buoy moved in an outward spiral from the center of the gyre during the first 7 days (fig. 2).

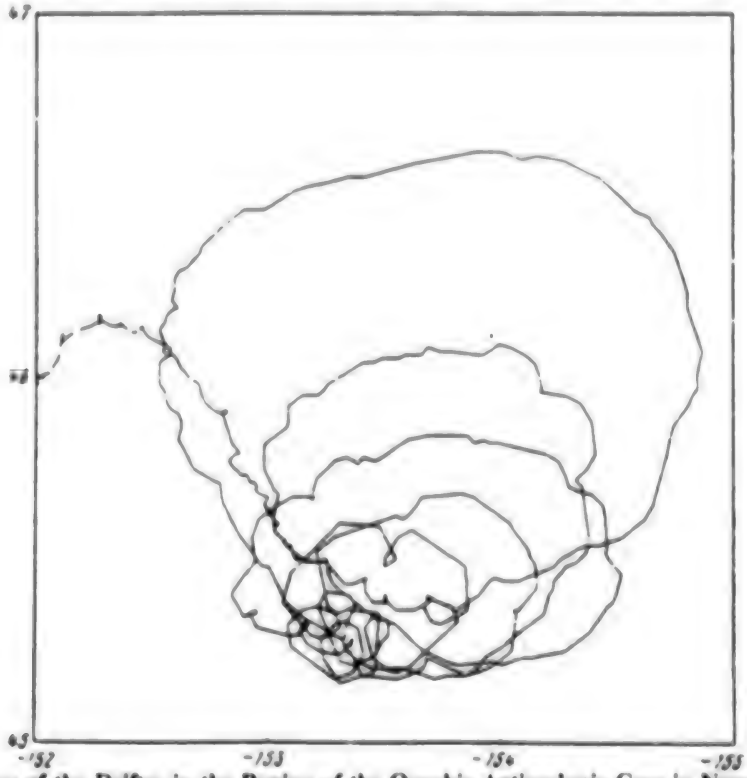

Fig. 1. The Trajectory of the Drifter in the Region of the Oyashio Anticyclonic Gyre in November-December 1990. The Longitude Is Along the X-Axis and the Latitude Is Along the Y-Axis.

4. The theoretical period of inertial oscillations is given by the expression:

$$T = 2\pi/(2\omega\sin\varphi),$$

where φ is the latitude and $\omega = 0.729 \times 10^{-4}s^{-1}$ is the angular velocity of the Earth's rotation. In the absence of relative vorticity, the period of inertial movement should be 16.93 hours for an average buoy location latitude of 45°. At the same time, the observed frequency of oscillations was markedly lower than the theoretical inertial frequency, and within the first 7 days coincided with the period of the daily tide. The difference between the theoretical and observed frequencies may be explained by the relative vorticity created by the anticyclonic gyre.

The effective Coriolis frequency replaces the Coriolis parameter value as the maximum lowest frequency of near-inertial movements. For spiral near-inertial waves, which are spreading in a gyre rotating with an angular velocity Ω, the approximate dispersion ratio may be written in the form:

$$(1)\ \omega_o = f_1 + (g/2f\rho)(\delta\rho/\delta z)(k)\,nfh/k_z)^2 + (g/f\rho)\delta\rho/\delta r\ k/k_z,$$

where $f_1 = f + 2\Omega$ - the effective value of the Coriolis parameter (this value includes the relative vorticity of the gyre), $g/\rho_o\delta\rho/\delta z$ is the buoyancy frequency, g is the free fall acceleration, ρ is density, z is the vertical coordinate, $k^2_h = k^2 + m^2/r^2$, k, m/r and k_z are the radial, azimuthal, and vertical wave numbers, r is the radius, $\omega_o = m\Omega - \omega$ is the internal frequency of spiral waves, ω is the frequency, and $m\Omega$ is the Doppler frequency shift. From the ratio (1) it follows that the internal frequency of the near-inertial waves can be reduced for an anticyclonic gyre ($\Omega < 0$). For a gyre rotation period of 5 days, the effective period of near-inertial spiral waves in the gyre (close to the value $f + 2\Omega$) will be 23.56 hours. Therefore, the period of the daily tide will coincide with the inertial period if the water in the gyre rotates with a period of 4-5 days.

5. Observations of the behavior of the drifter showed that elevated amplitude near-inertial movements as compared with the high frequency oscillations in the following period occurred when the inequality in the height of the tide is at its daily maximum in the area being researched. On the basis of this, it can be surmised that near-inertial movements of the buoy with a period close to the tide period were generated by the daily tide. Moreover, the area in which the buoy was placed is a region with irregular daily tides, which additionally confirms this supposition.

The connection identified between the internal dynamics of the Oyashio anticyclonic gyre with near-inertial movements having a period close to the tide period allows us to examine tides as one of the fundamental sources of energy necessary for mixing the nucleus of the gyre and generating the energy of turbulence.

In the work (4) a high level of kinetic energy dissipation under the nucleus of the anticyclonic gyre (the level exceeds typical values by a factor of two at the same depth in the Sargasso Sea) was explained by the generation of energy by near-inertial waves. Knowing the speed of kinetic energy dissipation and the total energy of the gyre, it is possible to evaluate its lifetime. Since a portion of this near-inertial wave energy can leave the gyre, such an evaluation of the lifetime of the gyre will be elevated. On the other hand, the exceptional duration in the life of the WCR86B presumes the presence of a constant source of energy for its existence. In fact, the WCR86B continued to move along the Kurile-Kamchatka channel at the end of 1991, which means the length of its existence can be counted at more than 5 years. Lueck and Osborn (4) evaluated the lifetime of a gyre at 3-4 years in the Sargasso Sea on the basis of the speed of dissipation of the kinetic energy. However, the tide mechanism for generating near-inertial movements in the Oyashio gyre assumes the existence of a constant source of energy. Due to the regularity of this mechanism, the lifetime of the gyre is extended. Since the tide near-inertial movements do not extract the mean kinetic energy of the gyre, assessments of lifetime based on the speed of dissipation are underestimated.

6. On the basis of an analysis of the trajectory of a surface drifter placed in the Oyashio anticyclonic gyre, near-inertial movements of large amplitude were determined. The theoretical inertial period was less than the observed period of near-inertial movements. An increase in the inertial period was observed in the central part of the gyre. Based on the theory of spiral near- inertial waves, an increase of the inertial period in an anticyclonic gyre is predicted due to the relative vorticity created by the gyre. The effective inertial period is close to the tide period which prevails in the region. Thus, near-inertial movements were generated by the action of the tide when they resonated with the daily tide. Therefore, the cited observations give a foundation to think that the anticyclonic gyre Oyashio receives additional energy from the action of the tide.

The surface drifter was furnished by the scientific research ship "Academician A. Vinogradov" for the Canadian program BOCE for researching surface currents. We are grateful to professor P. Le Blon from the University of British Columbia for providing information on the trajectory of the buoy and allowing us to use it in this article.

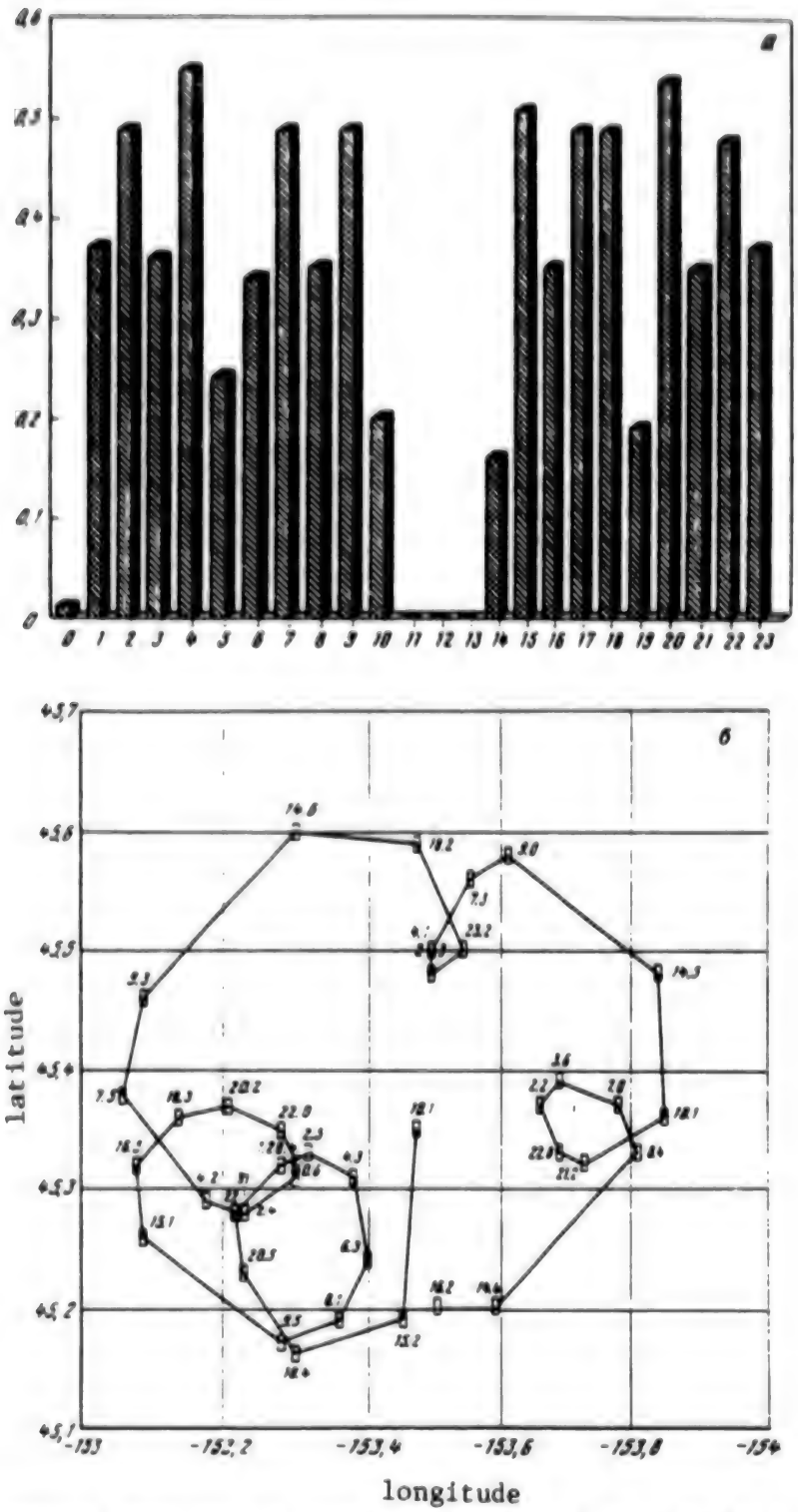

Fig. 2. (a) The Frequency of Determining the Drifter in a 24 Hour Period; Hours of the Day Along the X-Axis and Frequency of Determining Drifter Location Along the Y-Axis (Number of Determinations Per Hour). (b) Near-Inertial Drifter Movements in the Central Portion of the WCR86B Anticyclonic Drifter

The numbers by the marks are the time of day (hours and tens of minutes; longitude is along the X-axis and latitude along the Y-axis.

Footnotes

1. V. I. Ilichev, V. B. Lobanov, K. A. Rogachev, DOKLADY AKADEMII NAUK [Reports of the Academy of Sciences], vol. 308, pp. 1224-1227.

2. K. A. Rogachev, OKEANOLOGIYA [Oceanology], 1989, No. 6, p. 960.

3. K. A. Rogachev, V. A. Goryachev, *J. Geophys. Res.*, 1991, No. C5.

4. R. Lueck, T. Osborn, *J. Geophys. Res.*, 1985, vol. 91, No. C1, pp. 803-818.

Multi-Beam Echo Sounder for Deep Water

937F0057B Moscow OKEANOLOGIYA in Russian
No 5, 1992 pp 966-969

[Article by K. V. Avilov, S. A. Dremuchev, V. V. Krasnoborodko, V. G. Selivanov; UDC 534.6.08: 551.463.26]

[Text] This article describes a new type of multi-beam echo sounder, developed in the Russian Academy of Sciences Institute of Oceanology and installed on the "Mezen" scientific research ship. The use of a multi-channel (128 channels) analog-to-digital converter and a digital beam generator with an IBM PC AT is an important feature of the system being described.

The multi-beam echo sounder is designed for echo sounding of the sea bottom in order to obtain detailed information about its surface. At depths up to 6000 meters, the multi-beam echo sounder can be used to map the relief of the bottom at a specific width in the direction of the ship, measure the level of backward scattering of the signal at various angles, locate and determine the size of objects both within the middle of the water as well as on the surface of the bottom, and map the sea bottom in geographic coordinates. Moreover, the multi-beam echo sounder can be used as a side-scan sonar system, as well as a narrow beam echo sounder. Such broad possibilities of the device allow it to be used as a precision instrument for detailed cartographic surveying of the sea bottom, for highly accurate depth measurements, and for locating underwater objects, minerals, the laying of cables, etc. The combination of extreme accuracy and speed of the computer elements and the high degree of reliability of the analog devices makes this device a very effective means for acoustic research of the sea bottom by allowing results to be obtained in real time.

The drawing depicts a block diagram of the multi-beam echo sounder. The multi-beam echo sounder can be divided into three parts: transmitter portion, receiver portion and the computer system for processing and displaying the information.

The transmitter portion contains an antenna array, power amplifiers, and the pitch and timing compensation devices.

The receiver portion contains an antenna array, amplifiers, band-pass filters, multipliers, low-pass filters, and an analog-to-digital converter (ADC).

The computer system contains an IBM PC AT computer (the IBM PC XT may include software), an array processor, display, printer and plotter.

The multi-beam echo sounder functions in the following manner.

The radiating antenna array sends a short acoustic signal vertically downward. This signal is reflected from the bottom and received by the antenna array. The signal which is received is amplified, filtered, converted, digitized and sent to the computer. The computer and the array processor jointly process the received information mathematically and build a picture of the acoustic field reflected from the bottom. In order to achieve angular resolution of the reflected signals, the receiver portion of the computer is multi-channel.

The receiving antenna contains three linear arrays mounted across the ship, parallel to each other at a distance of one half the length of a wave. The distance between the receivers in the arrays is also equal to half the length of a wave. The length of the antenna is three meters. The width of the antenna pattern is approximately 2° in a plane perpendicular to the motion of the ship. The directional pattern along the ship is equal to 60°. A radiating antenna of similar design is mounted along the ship and its pattern is crossed with the pattern of the receiving antenna. These antennas help to obtain information about bottom area S with angular measurements of 2 x 2 degrees.

If several receiving beams are formed, which is what many foreign firms do, information can be received simultaneously on separate, elementary bottom areas, the number of which is equal to the number of receiving beams which are formed. For example, the Holming Electronic firm developed a multi-beam echo sounder with 15 beams, formed in a similar manner. Further, each beam is oriented to a specific angle and has a separate receiver channel. This echo sounder is different because separate beams do not form in it, but what occurs is expansion into a Fourier series along the space-wave vector. In this way, the current spacial spectrum of the dispersed signal strength is located in the receiving antenna aperture plane, independent of time (1-3). This method makes it possible to obtain a stereoscopic acoustic image of the bottom relief. Further, the number of equivalent receiving beams in the image is not limited by anything and can reach several hundred, while the number of independent beams is limited by the number of receivers in the array. This method of processing signals is equivalent to a system of 64 beams and up, and allows the electronic equipment to be simplified.

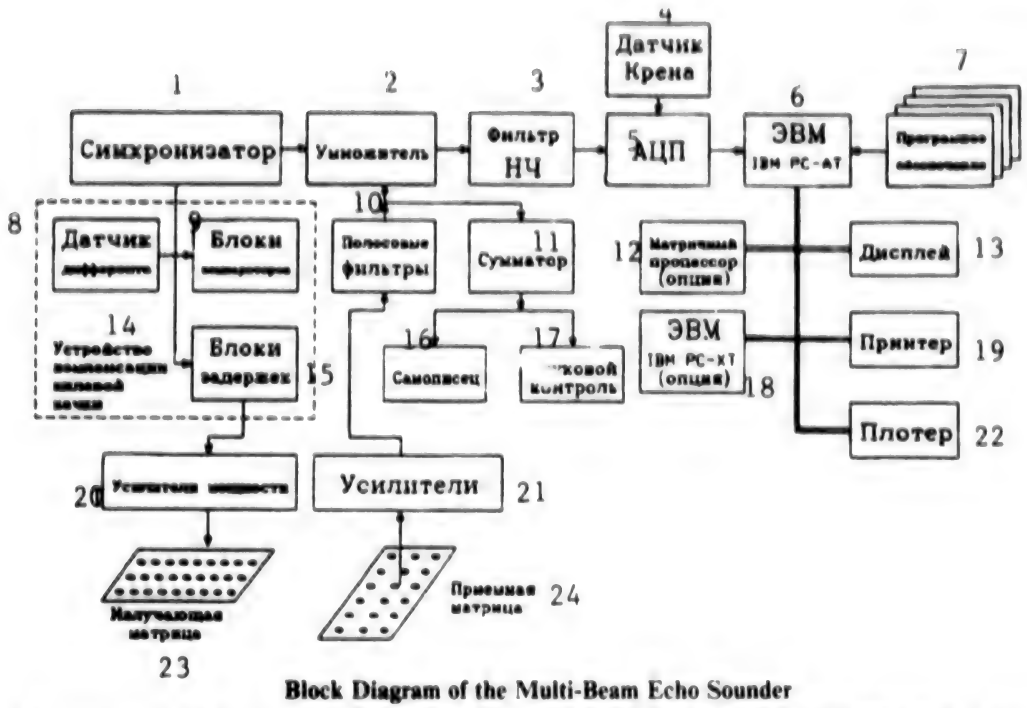

Block Diagram of the Multi-Beam Echo Sounder

Key: 1. Synchronizer; 2. Multiplier; 3. Low-Pass Filter; 4. Heeling Sensor; 5. ADC; 6. IBM PC AT; 7. Software; 8. Trim Sensor; 9. Comparator Units; 10. Band-Pass Filter; 11. Adder; 12. Array Processor (option); 13. Display; 14. Pitching Compensation Device; 15. Delay Units; 16. Recorder; 17. Sound Control; 18. IBM PC XT (option); 19. Printer; 20. Power Amplifiers; 21. Amplifiers; 22. Plotter; 23. Radiating Array; 24. Receiving Array.

Let us now turn to a more detailed examination of the block diagram of the multi-beam echo sounder.

The synchronizer sets the operating mode. It is stabilized by a 1 MHz quartz. Division is used to separate the 15625 Hz carrier frequency of the echo sounder. This frequency value provides for effective reflection of the acoustic signal from the bottom. Pulses with durations of 1, 2, 4, 8 and 16 microseconds and pulse spacing of 2.1, 4.2, 8.4 and 16.8 seconds are formed by division of this frequency. These values can be manually set by the operator.

In order to operate the multi-beam echo sounder when there is pitching, a compensation device is available. Let us say that the radiating antenna deviates from horizontal by angle α. So that the antenna radiates vertically, i.e., the wave front is cophased in a horizontal plane, a delay in radiation is introduced in each transmitting element of the antenna. The magnitude of the delay for the n element of the antenna is expressed in the form $T_n = (n - 1)/(N - 1)[D\sin\alpha]/c$, where D is the length of the antenna, α is the angle between the antenna and the horizontal plane, c is the speed of sound in water (1500 m/s), and N is the total number of elements in the antenna.

The device has 27 comparators and 27 delay units (equal to the number of radiating channels), which are used to generate the necessary delays proportional to the pitching signal. A signal proportional to the angle of pitch is sent to the first input via the weighing divider $(n\text{-}1)/(N\text{-}1)$. ..vtooth voltage from the synchronizer is sent to the second input. When the two voltages are compared, a pulse corresponding to T_n is generated at the comparator output. If their is no pitch, all pulses appear at one time and the antenna radiates perpendicular to its plane. If there is pitch, pulses appear at various times proportional to the signal of pitch and the weighing dividers. The pulses are sent to the delay units, where probing pulses of the 15625 Hz carrier frequency are formed at the leading edge from the 1 MHz reference frequency, so that the carrier frequency begins from the zero phase on all radiating channels. The duration of the probing pulses is also determined by the delay units and corresponds to the value established by the operator.

The probing pulses are transmitted from the delay units to the power amplifiers. Attached to each of the 27 delay units are three amplifiers, according to the number of transducer arrays in the row. Each strip of the amplifier is powered from a separate source. By managing how the sources are turned on, it is possible to regulate the output power of the multi-beam echo sounder. The amplifiers are loaded on piezoelectric ceramic transducers and each is tuned to resonate for its radiator, which is especially important for the integrity of the directional pattern.

The signals which are received by the antenna array are amplified by 40 dB by 60 amplifiers installed in a compartment of the receiving antenna. Subsequent amplification to 100 dB takes place in the filter units, where the signal passes through the band-pass filters with a band of 14-17 kHz. Further, the gain is set manually by the operator, depending upon the magnitude of the signal which is received. The units contain overload indicators in the light-emitting diodes. This allows the level of the received signal to be regulated. Then the signals which are filtered out and amplified are multiplied into two signals of the reference carrier frequency, and are moved out of phase by 90°. The reference signals are sent from the synchronizer. As a result of being multiplied together, the sum frequency is filtered out by a low-pass filter, and the variable frequency is isolated at the output of the filters. Since the radiated and reference frequencies are generated by one quartz generator, quadrature components of the input signal appear at the low-pass filter output, i.e., its sine and cosine components.

These signal components are "slowly" changing voltages (in comparison to the carrier frequency), in which information on the relief of the bottom is placed. The more indented the relief is, the more unstable the phase of the reflected signal. The more frequently readings of the input signal values are taken, the greater the resolution of the range system. This system uses an analog-to-digital converter with a sampling rate of 2 kHz along 128 channels simultaneously. Therefore the cut-off frequency of the low-pass filter is selected to be 2.5 times less at 700 Hz. It is apparent that such signal conversion not only makes narrow band filtration possible, but also markedly reduces the sampling rate of the analog-to-digital converter, which is especially important for multi-channel devices.

Signals digitized by the analog-to-digital converter are sent to the IBM PC AT computer. The computer controls the operation of the analog-to-digital converter and carries out Fourier transformation along the 128 channels, after which spectra are built in the coordinates depth-direction-intensity. The computer then determines the times of beam input, and it maps the relief and outputs it to the display. BPF, a specially developed, highly effective program, allows each probing pulse to be processed in real time on an IBM PC with a clock rate of 16 MHz and higher.

The second IBM PC XT computer uses the output data of the first computer to build bathymetric charts in geographic coordinates which are then output to the printer or plotter.

In order to regulate the operation of the echo sounder, there is a sound control channel. Signals which have passed through the pass-band filters are summed along all receiving channels, allowing for the phase, thus creating a narrow beam directed along the perpendicular to the antenna plane. This channel has a signal/noise ratio which is the square root of 60 higher than a single one. After additional filtration and conversions, the signal is transmitted to a loudspeaker. This channel can be used jointly with the depth recorder as an analog narrow beam echo sounder.

In order to eliminate the influence of on-board pitch, a signal from the heeling sensor is input. Before Fourier transformation, the computer inputs delays to the appropriate receiving channels. These delays are proportional to the sensor reading.

The multi-beam echo sounder, which was manufactured with the participation of other organizations, has undergone preliminary testing in the Pacific and Atlantic Oceans. The results which were obtained completely confirm its operability.

Footnotes

1. L. M. Brekhovskikh, V. V. Krasnoborodko, V. X. Kiriakov, V. G. Selivanov, "Obtaining Acoustical Imaging of the Sea Bottom by Using Multi-Element Antennas," USSR DOKLADY AKADEMII NAUK [USSR Reports of the Academy of Sciences], 1985, vol. 283, No. 4, pp. 1000-10002.

2. A. N. Bogdanov, V. V. Krasnoborodko, "Obtaining an Acoustic Stereoscopic Picture in the Ocean by Using a Multi-Element Planar Antenna," OCEANOLOGIYA [Oceanology], 1991, vol. 31, No. 1, pp. 170- 174.

3. A. N. Bogdanov, V. V. Krasnoborodko, Yu. P. Lysanov, "Synchronized Determination of the Characteristics of the Bottom Relief and Dispersal of Sound by Using Multi-Element Antennas," AKUSTICHESKIY ZHURNAL [Acoustic Journal], 1991, No. 2, pp. 246-250.

Ministry Holds News Conference on Spent Nuclear Fuel Problems

PM1611111392 Moscow Russian Television Network in Russian 1100 GMT 12 Nov 92

[From the "Vesti" newscast: Video report by M. Sarbaa, identified by caption, from Ministry of Nuclear Power Generation]

[Text] [Sarbaa over video of news conference] A news conference devoted to problems pertaining to spent nuclear fuel from nuclear power stations was held at the Russian Ministry of Nuclear Power Generation today.

A large proportion of the spent fuel is processed at a special plant in Chelyabinsk. Nuclear fuel from East European countries and Finland is processed at Chelyabinsk-65.

We learned at the news conference that difficulties have arisen with the transportation of nuclear fuel via CIS countries. Negotiations with a view to settling this question are under way.

Russia receives $800 per kilogram of nuclear fuel to be processed. A total of 60 tonnes are processed in Russia. A nuclear waste storage facility is located in Krasnoyarsk. There are many other nuclear sites in Russia. Most of them belong to the military department. The time has come to build a new deep nuclear burial facility. It will be built taking account of the public's wishes on the basis of the new law on nuclear waste. [video shows news conference, unidentified nuclear power station, interior of nuclear fuel processing plant]

Deputy Nuclear Power Minister on Disposal of Spent Nuclear Fuel

LD1311103292 Moscow ITAR-TASS in English 1328 GMT 12 Nov 92

[By ITAR-TASS correspondent Anna Bakina]

[Text] Moscow, November 12 (TASS)—"Disposing used fuel from nuclear power stations without reprocessing is hazardous for the life of succeeding generations," Russian Deputy Minister of Nuclear Power Nikolay Yegorov told a press conference here today.

Used fuel contains such radioactive substances as uranium and plutonium. During reprocessing they are separated and can be used again while the resulting waste should be kept in ground storage facilities for tens of years and then buried in underground tanks.

There is a well-developed nuclear fuel reprocessing network in the world. For instance, Britain and France accept Western Europe's used fuel. Russia reprocesses the fuel of the former socialist countries and Finland where nuclear power stations were build at one time under the Russian blueprint. Reprocessing is very costly. Countries that supply used fuel pay for this work in freely convertible currency, which certainly is one way to replenish the state budget.

Specialists at the Ministry of Nuclear Power say relationships with former Union republics, specifically Ukraine, are a major problem. For the present, the reprocessing by Russia of Ukraine's used fuel is paid under old agreements, in roubles. However, the political situation calls for the adoption of new legislative acts regulating interaction between former Union republics which are now sovereign states.

A special bill is currently elaborated in Russia to solve radioactive waste management problems. The bill is now under consideration in the Russian Government. This document has one more significant innovation: In case a question on disposing used fuel in some or other area is raised, the bill stipulates that the issue is put to a wide popular debate.

Ministry Admits Tver Nuclear Units' Design Flaws

LD2011195092 Moscow ITAR-TASS in English 1451 GMT 20 Nov 92

[By ITAR-TASS correspondent Veronika Romanenkova]

[Text] Moscow, November 20 (TASS)—The State Council of Experts of the Russian Ecological Ministry acknowledged today that the design of the second stage, including power units three and four, of the nuclear power stations in Tver (formerly Kalinin) "does not have sufficient ecological guarantees". Specialists think it is impossible to commission the third power unit without first solving a whole series of problems, the most important of which is water supply.

The 1984 design to expand the nuclear station in Tver to 4000 megawatts will be fullfilled by Nizhnyy Novgorod scientific researchers and designers of the Atomenergoproekt (Atomic Energy Design) Institute by order of the station's director.

Experts, following state orders, will examine the ecology in the area.

Murmansk Region Nuclear Waste Site Revealed

LD2211023092 Moscow Teleradiokompaniya Ostankino Television First Program Network in Russian 2100 GMT 21 Nov 92

[From the "Novosti" newscast]

[Text] It would appear that there are no more mysteries surrounding the problem of dumping nuclear waste. However, this is not so. None of the official sources mention a nuclear waste burial site in Andreyeva Guba in the Zapadnaya Litsa region of Murmansk Oblast. We have often mentioned that the nuclear waste situation on

the Kola peninsula is catastrophic. The atomic icebreaker fleet and Northern Fleet are unable to cope with this problem on their own. That is probably why unreliable nuclear waste burial sites are being built randomly on the Barents Sea coast. Today, there are over 100 atomic submarines waiting to be broken up for scrap. A wrangle is going on among deputies as to where their nuclear burial site is to be; meanwhile, dumps are being built. If there is a secret that may damage human lives, it is a criminal secret. Nuclear burial sites at Novaya Zemlya have been made public today, albeit late in the day. The news of a nuclear dump built in the Motovskiy Gulf in Andreyeva Guba may also come too late.

The health of the naval personnel working on the site is now at risk; but it is a disaster for us all, since this installation carries no guarantees of safety. [Video of site; people in protective clothing working inside an installation, a ship sailing at sea, aerial view of a harbor, military vessels, and an icebreaker.]

Committee Created To Retrieve Buried Nuclear Waste

LD0112163292 Moscow ITAR-TASS in English 1315 GMT 1 Dec 92

[By ITAR-TASS correspondent]

[Text] Moscow, December 1 (TASS)—Russian President Boris Yeltsin signed a decree creating a special committee which will engage in retrieving chemical ammunition and radioactive waste buried underwater, salvaging sunk combat hardware, as well as in averting ecological catastrophes on the water, according to the presidential press service.

The decree is called "On the Creation of the Committee on Special-Purpose Underwater Works at the Government of the Russian Federation". It appeared because of quite a few catastrophes which have taken place of late and resulted in violation of ecological stability in Russia and neighbouring states, the press service said on Tuesday.

Finnish Experts Draft Nuclear Safety Plan

937F0033A Helsinki HELSINGIN SANOMAT in Finnish 7 Oct 92 p 5

[Article by Jukka Perttu: "Deficiencies in Monitoring Safety Devices at St. Petersburg Nuclear Power Plant. Finns Have Already Installed Satellite Transmitters in Sosnovyy Bor"]

[Text] The Finnish experts who visited the Sosnovyy Bor nuclear power plant recommended that testing the condition of the pumps and valves in the plant's safety system be intensified.

Ilari Aro, a senior inspector from the Radiation Safety Center, said that while it was true that the operational effectiveness of the apparatus is being tested, the inspections are not on the Western level. They do not reveal the wear of the safety devices sufficiently well.

The Finns who studied the plant's operations for three weeks left a total of 10 proposals for the installation. Among other things the maintenance of the buildings should put more effort on cleaning, so that radioactive dirt does not contact the workers in the facility.

A Fire in the Turbine Room Would Endanger Control Room

In the opinion of the experts, however, the operation, maintenance, and monitoring of the most important systems are well-organized from the standpoint of the safety of the Sosnovyy Bor power plant.

Experts experienced in fire safety would like to reduce the risk of starting a fire in the turbine room and also to increase the firefighting capacity, since systems needed for cooling the reactor are in that room.

Last fall a fire raged in the turbine room of Chernobyl's No. 2 unit in which, among other things, the roof collapsed and damaged the reactor's cooling system.

In addition the control room of the Sosnovyy Bor power plant is located next to the turbine room, and a bad fire there would force the control room personnel, who control the plant, to flee.

At least twice the outbreak of fire in a turbine room has driven employees out of the control room in the territory of the former Soviet Union.

At the Sosnovyy Bor power plant their own fire safety improvement program is under way.

Difference in the Effectiveness of Inspection Devices

The capability of the Russian inspection devices to discover defects in welded seams has proved to be clearly inferior to that of Western equipment. It is planned to send Western devices to Russia.

The pipes that were inspected by the Finns at Sosnovyy Bor were in good condition. The sample was rather small, however.

Communications Satellite Hovers in the Sky

On Monday people are departing from Finland to install facilities for setting up satellite communications between Finland and Sosnovyy Bor. The power plant officials have the right to report occurrences to Finland on their own. The devices are easy to operate, an engineer learns to use one in a quarter hour.

A message is sent when a button is pushed and is transmitted via satellite to the Finns automatically in English.

The transmitter is a satellite of the Inmarsat system. The owners are members from over 60 countries, including Finland.

The satellite is parked at the equator over the South Atlantic Ocean. The message is received in Denmark, where it is transferred to the telex network and then on to Finland, Denmark, Norway, Sweden, Germany, and to the Moscow officials.

In Finland the telex is received by the Radiation Safety Center and the Weather Bureau.

Imatran Voima Will Install Electric Heaters in Kola

Satellite communications are coming to the Kola nuclear power plant, Polyarnyye Zori, too.

Imatran Voima has completed a six-point program through which the safety of the four nuclear units in Kola will be improved. In October the company will begin to install electric heaters for the emergency water storage tanks of units three and four, for example.

If the reactor is cooled with water that is too cold, cracks may be formed.

Foreign Exchange Worth 85 Million

Implementing the program will require foreign exchange valued at 85 million markkas in addition to the ruble financing. Financing is the responsibility of the Russians.

Norway has granted 20 million kroner for fixing up the Kola power plants. In Finland's budget for 1993 the Ministry of Commerce and Industry has set aside 12 million markkas for cooperation in the nuclear safety area with the countries of Central and East Europe.

Lapland's Water Supply Is Not in Danger

A nuclear power accident in Kola will not threaten Lapland's water supply, according to the Radiation Safety Center. The accident's dangers derive from the fact that radioactive substances are transported into the organism through the respiratory system and along with food. In addition outside radiation is detrimental.

It is stated at the Radiation Safety Center that at the worst drinking water could have 100-1,000 becquerels per liter. The use of water need not be restricted there, however.

Cesium is not transported into the ground water, and strontium too remains very strongly in the strata of the earth.

Examination of Energy Characteristics of Hydroelectric Power Plant-Pumped Storage Hydroelectric Power Plant Generating Unit Model With Capsule Set

937F0073A Moscow TYAZHELOYE MASHINOSTROYENIYE in Russian
No 9, Sep 92 pp 16-18

[Article by V.I. Vissarionov, V.V. Yelistratov, S.P. Serebryannikova, Ye.P. Machikha, Moscow Energy Institute, St. Petersburg State Engineering University, and Kharkov Turbine Plant; UDC 621.311.21.001.69]

[Abstract] The issue of upgrading existing hydroelectric power plants (GES) and using them during the low demand hours (at night) as pumping units for pumped storage hydroelectric power plants (GAES) is considered and it is speculated that the best effect can be attained by using GES with capsule units and linked upstream and downstream reservoir walls. The results of energy studies of a GES generating unit model with a capsule set carried out at an experimental test bench of the Renewable Energy Source and Hydroelectric Engineering Department at the St. Petersburg State Engineering University together with the Turboatom Production Association for the purpose of determining the operating and universal characteristics of the GES unit with a horizontal capsule set in the turbine and pump mode are reported. The experimental unit consists of a DC motor and a capsule set with two types of mass-produced impellers—the blade system of the OP-6 pump and PL-984 turbine. A conical nozzle with 20 vanes whose axes are sloping at 56° is used. An analysis shows that for series of hydroelectric power plants with linked reservoirs, the development of generating equipment which ensures operation in the GES-GAES mode is expedient. Optimum impeller blade characteristics are suggested for reversible operation of GES units. The experimental data are processed on a microcomputer. Figures 4; tables 1; references 4.

Stem Turbine Response Under Emergency Power System Conditions

937F0073B Moscow TYAZHELOYE MASHINOSTROYENIYE in Russian
No 9, Sep 92 pp 19-22

[Article by A.V. Rabinovich, S.N. Ivanov, V.B. Novoselov, R.S. Faskhutdinov, V.D. Ivashov, Ye.V. Osipenko, Production Association of the Turbine Motor Plant; UDC 621.156-531.9]

[Abstract] The goals of emergency prevention in power systems and quick restoration of normal operating conditions are discussed and the problems involved in meeting these goals are formulated: preventing network overloads and system instability under emergency power balance disruptions; preventing asynchronous conditions in the case where the emergency automation systems (PA) are inefficient and stability is upset; ensuring an emergency frequency relief (AChR) of the detached energy-short system; automatically starting up and engaging the units in the separated power systems; and automatically disconnecting the separated units from the AChR after the frequency is restored. Two methods of solving these problems are proposed. In one, the tasks are divided into two parts solved separately, while in the other all problems are solved comprehensively using the emergency automation system. The details of the methods as well as their relative advantages and shortcomings are outlined and their respective automatic control systems are considered. Particular attention is focused on the hydraulic control systems (GSR) of steam turbines (PT) operating through a high-speed electrohydraulic converter. The characteristics of the steam turbine response in an emergency operation are analyzed and the requirements imposed on the steam turbine maneuverability and methods of meeting them are described. The issue of separating the electric and hydraulic parts of the control systems and the specific features of automatic control systems for these devices are summarized. For illustration, the T-250/300-240 turbine is considered in detail. Figures 5; references 14.

Energy Efficiency of Threshold Solar Radiation Converter Cascade

937F0067A Tashkent GELIOTEKHNIKA in Russian
No 4, Jul-Aug 92 pp 3-8

[Article by L.N. Bell, Yu.M. Shapiguzov, N.D. Gudkov, Plant Physiology Institute at Russia's Academy of Sciences imeni K.A. Temiryazyev; UDC 621.383:621.472]

[Abstract] The thermodynamic constraints on the efficiency of direct solar radiation — work conversion systems and the properties which are common to all converters, i.e., their transparency at frequencies below a certain threshold, are discussed and an attempt is made to demonstrate that the thermodynamic limit of energy efficiency of such threshold converters is determined by a formula derived under an assumption of total absorption at frequencies above the threshold. Here, efficiency is defined as the ratio of the power generated by the converter to the radiant flux incident upon it. It is speculated that by using a cascade of threshold converters one can expect a significant increase in the optimum threshold frequency. A block diagram of a cascade of several radiant energy threshold converter stages is cited and a formula is derived for the extremum value of the cascade's thermodynamically feasible efficiency.. The case where a Planckian radiation is incident upon the converter stage is considered and the thermodynamic maximum limit of optimum radiant energy converter stage efficiency as a function of the number of stages is examined. An analysis shows that the development of converter stage arrangements is a promising way of increasing the solar converter efficiency not only from the practical but also principal viewpoints. It is noted that the maximum energy efficiency of threshold circuit stages can also be calculated by other methods. As the number of stages increases, the limit of energy efficiency

of a multistage converter approaches the thermodynamic maximum yield of a single optically thick converter, i.e., 0.92. A single stage efficiency is close to 40%. Figures 2; references 8: 4 Russian, 4 Western.

Production Practices of Cast Secondary Polycrystalline Silicon and Solar Cells on Its Basis

937F0067B Tashkent GELIOTEKHNIKA in Russian No 4, Jul-Aug 92 pp 8-14

[Article by B.M. Abdurakhmanov, T.Kh. Achilov, A.L. Kadyrov, Sh.T. Kasymov, M.S. Saidov, V.Ya. Tadzhiyev, M. Khalikov, S. Khoshimov, O.I. Chechetka, Electronics Institute at the Uzbek Republic Academy of Sciences imeni U.A. Arifov; UDC 621.383:537.215]

[Abstract] The high cost of single crystal silicon (MK) solar cells (SE) and the problem of increasing the use of polycrystalline silicon (PK) due to the need for large quantities of raw silicon prompted an investigation into the possibility of commercial production of polycrystalline silicon-based solar cells by utilizing all types of raw silicon, single crystal silicon, and electronic industry product (IET) waste. Attention is focused on a simple and large-scale method of polycrystalline silicon production on the basis of raw and single crystal silicon waste which are free of deep lying impurities and whose specified electrophysical characteristics acceptable for solar cells can be attained by special doping. A block-diagram of solar cell production on the basis of secondary cast polycrystalline silicon, including silicon single-layer epitaxial structures (KOES), is cited and the experience of secondary cast polycrystalline silicon (VLPK) production in Tadzhikistan using DMTsK-3TKh units originally designed for making silicon arrays is outlined. The parameters of various types of 2x4 cm solar cells on the basis of secondary cast polycrystalline silicon is summarized and the specific methods of developing secondary cast polycrystalline silicon substrates for solar cells, *p-n*-junctions, and front and rear solar cell contacts are described. The procedures for taking electrophysical measurements and the characteristics of secondary cast polycrystalline silicon solar cells are discussed and the dependence of the Hall mobility on the doping level in various solar cell materials is plotted. The relationship between the yield of suitable solar cells and their efficiency on the one hand and the cell size on the other is described. The outlook for using secondary cast polycrystalline silicon for concentrated solar radiation (KSI) systems is assessed. Figures 3; tables 4; references 18: 15 Russian, 3 Western.

Ways of Increasing Solar Cell Stage Power

937F0067C Tashkent GELIOTEKHNIKA in Russian No 4, Jul-Aug 92 pp 14-18

[Article by M.A. Abdukadyrov, Kh.Kh. Bustanov, M. Mirzabayev, Engineering Physics Institute and Sun-Physics Scientific Production Association at the Uzbek Republic Academy of Sciences; UDC 621.383:535.376]

[Abstract] The constantly rising interest in direct solar → electric energy conversion by semiconductor solar cells and the need to find new semiconductor materials and heterosystems on their basis for improving the photoelectric converters' energy indicators helped focus attention on the use of multijunction multistage solar cells (KSE) with a serially connected wide-and narrow-band separating barriers and using concentrators and double-sided exposure. It is speculated that from the viewpoint of multistage solar cell implementation, two-stage AlGaAs-Si solar cells are the most promising. Such composite multistage converters developed by the authors for single-sided direct and concentrated solar radiation conversion are outlined and their design and operating principles are described. The spectral distribution of the $Al_{0.15}Ga_{0.85}As$ and *p-n*-Si junction collecting coefficient in the stage as well some solid solutions are plotted. The principal parameters of the series connections of KSE stages, i.e., forbidden band, number of *p-n*-junctions per stage, no-load voltage, short circuit current, and output electric power at an optimum load, are summarized. An analysis shows that implementation of multistage cell models in solar power plants combined with solar flux and power concentration greatly improves the solar cell performance due to increasing the output voltage and power picked off from the active element unit area. Figures 3; tables 1; references 14: 12 Russian, 2 Western.

Photoelectric Converters With InP Heterojunction

937F0067D Tashkent GELIOTEKHNIKA in Russian No 4, Jul-Aug 92 pp 18-23

[Article by V.M. Botnaryuk, L.V. Gorchak, N.A. Grigina, M.B. Kagan, I.V. Karpenko, A.D. Kitoroaga, A.V. Koval, A.V. Simashkevich, Moldovan State University; UDC 621.362:621.383.5]

[Abstract] An attempt is made to verify experimentally the reports that an 18% efficiency has been achieved in InP-based photoconverters (FP) with a diffusion *p-n*-junction with hetero- and surface barrier structures with a photoactive area of 0.25-0.75 cm^2 under earth conditions. In addition, the issue of reproducing theoretical estimates and bringing the photoactive area of InP photoconverters to the level typical of devices on the basis Si and GaAs is addressed. To this end, photoconverters with an InP-CdS heterostructure produced on the basis of single crystal Czochralski-grown InP substrates are examined and their photoelectric characteristics are compared to those of InP-CdS heterostructures with a p^+-p^--n^+ structure produced with partial use of heterophase epitaxial technology. In all, the base InP component parameters at a 300K temperature of light batches with a (100) and (111)A structure, i.e., carrier concentration, resistivity, and mobility, are summarized. The light load characteristics of InP photoconverters with various structures, the dependence of the no-load voltage, short circuit current density, voltage-current characteristic filling factor (FF), and conversion efficiency of InP-CdS photoconverters, the InP-CdS

photoconverter spectral response as a function of the base component doping degree, and the light load characteristic of an actual photoconverter with a 5 cm^2 area are plotted. The latter FP's efficiency does not exceed 7.2%. The conclusion is drawn that although the efficiency of actual FPs is below theoretical estimates, an analysis of the dependence of photoelectric parameters on the doping degree shows that in using wafers with an InP doping of $p = (2\text{-}30) \times 10^{16}$ cm^{-3} with a 1 cm^2 working area, one can attain a 12.2% efficiency. The study demonstrates that for exoatmospheric applications, an 8.9% efficiency can be attained in 5 cm^2 FPs. Figures 4; tables 1; references 5: 1 Russian, 4 Western.

Solar-to-Chemical Energy Conversion in Photoelectrochemical Cell With $CdSe/TiO_2$ Photoanode

937F0067E Tashkent GELIOTEKHNIKA in Russian No 4, Jul-Aug 92 pp 27-30

[Article by A.S. Suleymanov, Inorganic and Physical Chemistry Institute at the Azeri Republic Academy of Sciences; UDC 541.13:621.135]

[Abstract] Ways of increasing the solar — chemical energy conversion efficiency using semiconductor heterostructures serving as photoelectrodes in electrolytic cells are discussed and it is asserted that semiconductors with a narrow forbidden gap and a wide-band oxide semiconductor applied to their surface are the best heterostructures for this purpose. It is speculated that the use of such heterostructures as photoanodes in a photoelectrochemical cell makes it possible, first, to protect the narrow-gap semiconductor surface from photostimulated corrosion; second, maximize the utilization efficiency of solar radiation; and third, greatly increase the conversion efficiency (KPD). To check these premises, an experiment is conducted: a TiO_2 film is used as the outer layer (protective film) and A2B6 and A3B5 compounds—as the narrow-band semiconductor (inner layer)—and the possibility of developing semiconductor heterostructures on the basis of TiO_2 and CdSe is studied and their electrochemical behavior during the photoelectrolysis of water is analyzed. The film production method and experimental technique are outlined. The anode polarization curves on TiO_2, CdSe, and $CdSe/TiO_2$, anodic photocurrent behavior on $CdSe/TiO_2$ and CdSe electrodes under the effect of light with $\lambda \geq 500$ nm in a sodium sulfate solution, the $CdSe/TiO_2$ anode potential behavior after turning off the prepolarization, under irradiation, and after irradiation, and the spectral dependence of the anode photocurrent on the irradiation wavelength at a +0.5 V electrode potential are plotted. An analysis shows that the titanium dioxide protective film may greatly inhibit CdSe photocorrosion and that solar radiation is absorbed more efficiently on $CdSe/TiO_2$ heterostructures than on individual components. It is mentioned that the hole transport mechanism from the narrow-gap semiconductor through the protective film toward the electrolyte-heterostructure interface will be considered in the next article. Figures 44; references 11: 5 Russian, 6 Western.

Generalized Planar Solar Collector Design Optimization Criterion

937F0067F Tashkent GELIOTEKHNIKA in Russian No 4, Jul-Aug 92 pp 31-34

[Article by V.B. Tarnizhevskiy, Yu.L. Myshko, V.V. Moiseyenko, State Scientific Research Energy Institute imeni G.M. Krzhizhanovskiy; UDC 662.997]

[Abstract] The issue of design optimization of planar solar collector elements, mostly the absorbing panels and rear heat insulation and the air gap between the absorbing panel and transparent insulation and the optimization criteria currently used for this purpose are discussed and the lack of studies of collector design optimization as a whole allowing for its most important application properties and cost factors is noted. The principal requirements determining the collector suitability for use are formulated: sufficient service life, low cost, and high thermal efficiency. Likewise, an attempt is made to select a single optimization criterion which can quantify uniquely and objectively the extent to which the collector meets these three conditions. As a result, a generalized optimization criterion is introduced as a ratio of the specific cost, in ruble/m^2, to the specific thermal yield during its service life, in kWh. The criterion, therefore, is measured in rubles per kWh and expresses the cost of a unit of power generated by the collector when user outlays are determined only by the fixed capital. The use of the new criterion is illustrated by a comparative analysis of three solar collectors. Tables 1; references 6.

Analysis of Findings of Study of Combined Photoelectric Collector With Mirror Concentrator

937F0067G Tashkent GELIOTEKHNIKA in Russian No 4, Jul-Aug 92 pp 34-37

[Article by V.I. Vissarionov, S.A. Bessonov, Moscow Energy Institute; UDC 621.362:537.215]

[Abstract] The shortcomings of solar radiation collectors used for lowering the cost of solar power plants, i.e., the need to remove additional heat from the photocells with the help of, e.g, water (which, incidentally, can be utilized for heating purposes) prompted an investigation into the use of a mirror concentrator with a combined photoelectric collector (KFK) manufactured by the Saturn Scientific Production Association. The combined photoelectric collector is a water-cooled silicon photoelectric battery with an area of 0.5 m^2. Accordingly, a mirror concentrator was designed and produced at the Moscow Energy Institute. It is shaped as a truncated pyramid with a concentration coefficient of 3. Mirrors with a 0.7 reflectance are installed on the pyramid faces; each face is detachable, making it possible to manipulate

the concentration coefficient. A battery with the combined photoelectric collector was installed in one of the solar units at the Crimean Solar Power Plant (SES) and an experimental study was conducted. The following operating conditions were examined: operation without cooling and concentration; without cooling but with concentration with a 1.5 and 3 concentration coefficient; and at a concentration coefficient of 3 at various water coolant rates. The voltage-current characteristics of the combined photoelectric collector under the above conditions are plotted and the curves are analyzed. The efficacy of using the combined photoelectric collector with the concentrator is confirmed and it is noted that the device may be improved further by replacing the mirrors with polymer films with a high reflectance, making it possible to increase efficiency and make the structure cheaper and lighter while increasing the cooling water temperature for use in other systems. Figures 3; references 1.

Convective Heat Transfer and Friction Loss in Solar Air Heaters With Corrugated Heat Absorbers

937F0067H Tashkent GELIOTEKHNIKA in Russian No 4, Jul-Aug 92 pp 37-40

[Article by M.K. Karabayev, Ye.S. Abbasov, Fergana Polytechnic Institute; UDC 662.997:621.472]

[Abstract] The problems which hinder the development of highly economic solar warm-air heating systems based on solar air heaters (SVKhN) with corrugated heat absorbers, particularly the difficulty of calculating the heat transfer coefficient and friction loss during the air movement along the heat exchange profile surfaces, and the lack of formulae for analyzing the thermal hydraulic characteristics of corrugated channels with various diffuser angles, prompted a study of the heat transfer and friction loss in solar heaters with corrugated heat absorbers. To this end, a diffuser-confuser system consisting of two 20 mm thick plates, one smooth and one grooved, and two transparent glass side walls is examined and the flow pattern is analyzed in the channel's third wave. The experimental procedure is outlined in detail and the model of heat transfer enhancement in the corrugated sun light absorber channel and the convective heat transfer and friction loss in the corrugated sun light absorber in the air flow are plotted. The findings are compared to analytical data and good consistency is noted within the entire Re number range. Figures 2; references 3.

Device for Assessing Mirror Surface Quality

937F0067I Tashkent GELIOTEKHNIKA in Russian No 4, Jul-Aug 92 pp 47-48

[Article by Yang Jingshe, Zang Yingsheng, Xinjiang New Energy Source Research Institute; UDC 662.997: 621.472]

[Abstract] A report presented to the First Sino-Soviet Solar Energy Seminar held in Tashkent in September, 1991 is summarized. The importance of specular reflectance (KZO) as a criterion for assessing the quality of reflecting surfaces is stressed and the shortcomings of existing methods of measuring it are outlined. A new device which is free of its predecessors' disadvantages is described. It consists of four parts. The integrating sphere contains two hemispheres made from an aluminum alloy; the inner sphere wall is covered with a thin $BaSO_4$ layer with MgO on top of it. Eight pairs of temperature sensitive elements encased in vacuum tubes are used as the detector and direct solar radiation serves as the energy source. Manual tracking which makes it possible to turn the device 360° around its axis is used. The light trap is made according to the aperture angle. The device was tested in measuring the specular reflectance of aluminum-coated PVC (PVKh) film. The specular reflectance increases with the aperture angle. The need for further studies and improvements in order to eliminate the effect of the weather factors on the measurement outcome is stressed. Figures 1; references: 1 Western.

Improving Passive Solar Heating System With Collecting Accumulating Wall

937F0067J Tashkent GELIOTEKHNIKA in Russian No 4, Jul-Aug 92 pp 54-56

[Article by K.N. Chakalev, Zh.D. Sadykov, State Scientific Research Energy Institute imeni G.M. Krzhizhanovskiy; UDC 662.997:697.1]

[Abstract] The linear dependence of the mean heating load substitution factor during the entire heating season on the product of the relative mean monthly ambient temperature (averaged over the same period) by the entity temperature and the mean monthly total solar radiation on a horizontal surface over the heating season derived earlier is discussed (*Geliotekhnika* No 4, Jul-Aug 89) and the next stage of the study is carried out: an attempt to examine the effect of the design modifications in the passive solar heating system and the heated entity using simplified formulae. It is speculated that the design modifications in the system can be expressed by a family of straight lines in the F-$H\theta$ coordinates. To check this assumption, the heating system substitution coefficient of the heating demand as a function of the number of glass paneling layers, the thickness and thermal conductivity of the collecting accumulating wall materials, and the nocturnal insulation installation is examined. An empirical dependence of the increase in the substitution coefficient with an increase in the wall thickness is derived and the dependence of the heating demand substitution coefficient on the wall thickness is plotted for the weather conditions in Ashgabat, Gasan-Kuli, Churuk, Bishkek, and Odessa. The outlook for using such analyses in determining the passive solar heating efficiency under varying climatic conditions and estimating the effect of architectural changes in the system is assessed. Figures 1; references 5.

Effect of Selective Absorbing Coat on Thermal Characteristics of Low- and Medium-Temperature Solar Plants

937F0067K Tashkent GELIOTEKHNIKA in Russian No 4, Jul-Aug 92 pp 68-71

[Article by Wang Guohua, Xinjiang New Energy Source Research Institute; UDC 662.997]

[Abstract] A report presented to the First Sino-Soviet Solar Energy Seminar held in Tashkent in September, 1991 is summarized. The use of the average daily efficiency and efficiency dynamics for characterizing the solar system collectors and the effect of various factors on this efficiency are discussed and an attempt is made to study the effect of selective absorbing coat on the thermal characteristics of low- and medium-temperature solar units. To this end, tests are carried out at 80°C and 200-300°C in order to optimize the coats used in different temperature ranges. It is noted that the solar energy conversion efficiency is directly proportionate to the sun light absorber's absorptance in the absence of convective heat transfer and conduction losses. An efficiency formula is derived and the correlation of the time dependence of the collector efficiency and the coolant and ambient temperatures, the quantity of solar radiation received, and the number of daylight hours per day is established and the effect of the selective absorbing coat is plotted and tabulated. The findings show that coats with a concentration coefficient of 3 have the greatest impact on the heating rate and the highest equilibrium temperature. It is noted that in the area of low temperatures, the collector characteristics depend primarily on the coat absorptance for solar radiation. The need to maximize the coat absorptance for solar radiation and minimize the coat's own emissivity is stressed. Figures 1; tables 5; references: 2 Western.

Self-Contained Power Supply Source

937F0067L Tashkent GELIOTEKHNIKA in Russian No 4, Jul-Aug 92 pp 72-74

[Article by M.Ya. Bakirov, Radiation Research Sector at the Azeri Republic Academy of Sciences; UDC 662.997.4]

[Abstract] The operating principles of a lab prototype of a combined self-contained electric power supply source consisting of three principal components—a solar battery, a solid polymer electrolyzer (TPE), and a fuel cell—are presented and certain characteristics of the unit are examined. The unit operates on the basis of a nontraditional principle of converting solar energy into electric, electric to chemical, and chemical back to electric. The design of the three power supply components is described and the voltage-current characteristics of the solar battery, electrolyzer, and fuel cell are plotted. The lab unit was tested under full-scale conditions in Apsheron and is characterized by its stability and operational reliability; it is easy to maintain and the settling time is short. Analyses show that such a 5 m^2 unit with a silicon solar battery, an electrolyzer with 500 cm^2 electrodes, and a 2 kW fuel cell can be used in southern CIS, primarily by field workers. The authors are hopeful that such combined units will become a part of the power industry infrastructure. Figures 2; references 3.

Effect of Power System Failures on Industrial Facility Condition

937F0092A Moscow NADEZHNOST I KONTROL KACHESTVA: SERIYA NADEZHNOST in Russian No 11, Nov 92 pp 29-37

[Article by Ye.M. Chervonnyy, B.V. Papkov; UDC 621.311.019.3]

[Abstract] The effect of power system failures on the condition of industrial facilities is considered against the backdrop of increasing power shortages and declining generating capacity of power plants coupled with the limited capacity of transmission lines and system-forming and intersystem links. The conditions for enabling the electric power systems (EES) to maintain their serviceability are addressed and the importance for industrial enterprises to be able to maintain production, albeit at a less economical level, with changes in the load curve instead of cutting back output and missing shipping deadlines is stressed. The resulting need for built-in redundancy with respect to electric power availability and for identifying individual units which can or cannot operate independently from each other at each installation is outlined. The above redundancy is quantified and the operation of an industrial enterprise with disconnected loads due to power shortages is illustrated. Real capabilities of decreasing the power demand of industrial facilities while maintaining their commercial production at a planned level are assessed and it is stressed that power limitations do not affect the outcome of industrial enterprise operation if the possibility of load shedding under emergency power shortages is incorporated in the plans and regulatory documents. The decisions made by power system dispatchers will make it possible to minimize process disruptions and the economic consequences of load curve variations. Thus, limiting power consumption standards must be developed by the enterprises on the basis of a thorough analysis of their functional capabilities. References 6.

Taking Into Account Service Life Factor in Large Pipeline System Design

937F0092B Moscow NADEZHNOST I KONTROL KACHESTVA: SERIYA NADEZHNOST in Russian No 11, Nov 92 pp 44-50

[Article by M.G. Sukharev; UDC 62-192:622.691+62-192:622.692.4]

[Abstract] The importance of system reliability, particularly for large pipeline systems (BTS), and the lack of unified interpretation of the concept of reliability and the shortage of data on this subject prompted an attempt to analyze long-term BTS system performance together with the installation under design. Such an analysis must include the following components: determining the installation's service life and changes in its function during its entire life, taking into account the fact that individual components are brought on stream at different times, determining the overhaul and equipment replacement times, and predicting the dynamics of reliability indicators allowing for equipment aging and diversity. Specific and specialized models are developed for solving these problems and two strategies of addressing the issue of redundancy are formulated. Pipeline production curves under both strategies are plotted and the probabilities of events which are likely to occur in a pipeline with ten pumping stations some of which have failed are summarized. The findings show that in designing main pipelines, the change in their functions over the lifetime of the system must be taken into account by adding the corresponding specifications to the standards. The specific features of the adjusted cost optimization criterion are considered and it is stressed that recommendations concerning the pipeline service life must be based on a sound comprehensive examination of the pipeline condition and take into account its future role in the system. The effect of various factors on the pipe and equipment longevity is assessed. Figures 1; tables 1; references 5: 4 Russian, 1 Western.

Highly Concentrated Coal Slurry: New Power Plant Fuel

937F0094A Moscow ELEKTRICHESKIYE STANTSII in Russian No 11, Nov 92 pp 33-39

[Article by V.P. Shorokhov, G.G. Bruyer, Krasnoyarskugol and KATEKNIIugol; UDC 621.867.72:662.33]

[Abstract] The unique and large brown coal deposits in the Kansk-Achinsk Basin and the favorable seam bedding combined with the deposit suitability for strip mining are examined against the backdrop of the special role assigned to the leading development of the country's energy potential in addressing the issue of socioeconomic development. The low ash, sulfur, and radionuclide content in the Kansk-Achinsk coal (0.2-0.4 pCi/g) combined with its relatively high calorific value make its use as fuel especially efficient. Yet this lignite's high moisture content complicates its shipment over long distances and necessitates the development of alternate methods. This factor together with the high cost of power lines make coal slurry transportation over underground pipelines to areas with high electric power consumption especially attractive. Thus, coal can be pulverized and pumped to thermal power plants enabling them to abandon the use of "dirty" fuels. The issue of developing a coal slurry pipeline infrastructure is addressed and the experience accumulated in this field, both in the CIS and abroad, is reviewed. It is noted that a total of 128 companies worldwide are involved in coal slurry pipeline and processing equipment development. The advantages of coal slurry uses are indisputable. The conclusion is drawn that construction of slurry pipelines and facilities is economically expedient. Plans for building such pipelines are outlined and the need to set up a special effort in the framework of the "Environmentally Clean Power Industry" program is stressed. References 6.

Elastic Wave Precession in Rotating Body

937F0086A Moscow IZVESTIYA AKADEMII NAUK: MEKHANIKA TVERDOGO TELA in Russian No 4, Jul-Aug 92 pp 3-6

[Article by I.V. Batov, B.P. Bodunov, M.N. Danchevskaya, V.M. Lopatin, B.S. Lunin, V.V. Filatov, M.Yu. Shatalov, V.Ye. Yurin, Moscow; UDC 531.38]

[Abstract] The history of elastic wave precession studies since its discovery by G.H. Bryan in 1890 is reviewed and the case of precession at a random dependence of angular velocity on time is considered. In particular, elastic wave precession in a rotating shell—a hemispheric quartz resonator with a 2.7 kHz natural frequency with electrodes glued to its walls for taking capacitive measurements—is examined. The wave precession rate is measured at a specified principal axes position and the main wave precession components, scale factor, and the effect of the angular velocity and Earth's rotation are determined. A precession model which takes into account the dependence of the precession rate on the wave's angular position is constructed. The measured scale factor between the wave rotation angle relative to the instrument and the instrument rotation relative to the inertial space is consistent with both earlier theoretical and experimental data. The constant component of the wave precession includes precession caused by the Earth's angular velocity and is the only model component which depends substantially on the instrument's orientation. Figures 3; tables 1; references 6: 3 Russian, 3 Western.

Effect of Rotating Body on Point Mass or Why Planets Do Not Fall on Sun

937F0086B Moscow IZVESTIYA AKADEMII NAUK: MEKHANIKA TVERDOGO TELA in Russian No 4, Jul-Aug 92 pp 7-15

[Article by Ye.F. Tomilin, Moscow; UDC 521.151]

[Abstract] The two-body problem with respect to the motion of planets revolving around the sun is considered in a new formulation which takes into account the celestial bodies' atmospheres and the existence of an extraneous force which compensates for the interplanetary gas drag is assumed; it is speculated that the sun is the only possible source of this force. The problem is solved by considering the effect of a rotating disc on a point mass and the effect of a rotating sphere on a point mass in an inertial system of reference allowing for the finite velocity of this interaction. The existence of a transversal component of the sun's effect on the planets is demonstrated and calculated and the orbital velocity and aerodynamic drag coefficients are summarized. The continuing counterclockwise revolution of the planets in the same plane and the very fact that the orbits exist despite the interplanetary gas drag are attributed to the transversal component of the sun's interaction force. The ecliptic passes through the equator of the sun which spins at the same time thus pushing the planets in the direction of their rotation. The author is grateful to Academician V.F. Zhuravlev for valuable advice and support. Figures 2; tables 1; references 12.

On One Solution Approximation of Kinematic Motion Equations of Rigid Body

937F0086C Moscow IZVESTIYA AKADEMII NAUK: MEKHANIKA TVERDOGO TELA in Russian No 4, Jul-Aug 92 pp 16-23

[Article by S.V. Sokolov, Rostov-na-Donu; UDC 531.73]

[Abstract] The applied problem of controlling the orientation of a rigid body as well as inertial navigation and initial gyro system orientation which call for integrating Euler's kinematic relationships are considered and an attempt is made to develop a unified approach to solving the system of kinematic equations and expand the domain of analytical representation of the solutions of the systems of kinematic equations to the description of the vector of instantaneous rotation speed in time with the help of various approximating forms which ensure the necessary accuracy of instantaneous speed definition. The formulated problem is solved in two stages: the solution of kinematic equations is represented as elementary trigonometric functions for a constant direction of the velocity vector; the approximating form of velocity notation is found, making it possible to describe the current orientation of the rigid body with the help of a finite or countable sequence of finite turns with a known rotation axis direction. The elementary functions are derived by expanding into series the matrix forms of the system allowing for the skew-symmetric matrix of the angular velocity. The method is illustrated by an approximate solution of the problem of finding the current orientation of a stabilized platform performing small angular motions under harmonic variations in the angular velocity assuming that the amplitude ratio of harmonic components to their frequency is much less than unity. It is shows that the above approach makes it possible to find a precise solution without these assumptions. The current orientation parameters thus found are indeed the precise solution of the problem over a random time interval. References 4.

On Spatial Collision of Rigid Bodies

937F0086D Moscow IZVESTIYA AKADEMII NAUK: MEKHANIKA TVERDOGO TELA in Russian No 4, Jul-Aug 92 pp 24-30

[Article by R.F. Nagayev, St. Petersburg; UDC 531.3]

[Abstract] The problem of impact interaction of rigid bodies in space are considered in a stereomechanical formulation and the equation of impulsive motion with slip is derived. It is shown that the dependence of motion parameters on time cannot be determined within the impact interval and an attempt is made to demonstrate that the problem of spatial collision of bodies can be extended to the case with anisotropic dry friction

between the contact areas. To this end, explicit inequalities sufficient for ensuring the slipping nature of collision are derived. Motion after the end of slip is examined and the hypotheses of stereomechanical theory of collision are discussed. The impact momentum restoration coefficient which characterizes the relative proportion of the work of the normal force in separating the colliding bodies is calculated. The conditions ensuring the possibility of extended contact or an instantaneous change in the slip direction are defined and impulsive motion at a constant slip velocity direction is analyzed. References 3.

On Equilibrium Control of Wall Climbing Robot

937F0086E Moscow IZVESTIYA AKADEMII NAUK: MEKHANIKA TVERDOGO TELA in Russian No 4, Jul-Aug 92 pp 58-70

[Article by N.N. Bolotnik, G.Ch. Chandi, Moscow; UDC 531.8]

[Abstract] The design, operating principles, and applications of wall climbing (vertical motion) robots and their magnetic and vacuum grip systems are reviewed and the equilibrium conditions of a wall climbing robot are investigated allowing for the control moments in the robot foot joints. The optimization problem of determining the robot foot position on the surface and the control moment distribution minimizing the degree of vacuum in the grip cavities necessary for retaining the robot in a specified position is formulated. The problem is solved for a stepping robot with a symmetric design under certain simplifying assumptions. A mechanical model of the wall climbing robot and its kinematic correlations and the robot equilibrium conditions on the working surface are considered in detail. Figures 3; references 9: 3 Russian, 6 Western.

On Eigenmode Dynamics of Rotating Axisymmetric Elastic Body

937F0086F Moscow IZVESTIYA AKADEMII NAUK: MEKHANIKA TVERDOGO TELA in Russian No 4, Jul-Aug 92 pp 99-105

[Article by Yu.G. Markov, I.V. Skorobogatykh, Moscow; UDC 539.9]

[Abstract] The dynamic properties of an elastic axisymmetric body with a free boundary in a medium assumed to be isotropic and homogeneous and having a constant density described by a model of linear theory of elasticity are considered and a system of coordinates with the origin at the center of mass is introduced to describe the elastic strain in the body. Elastic vibrations are excited in an originally stationary body and the problem of studying the effect of the system rotation as a whole around a random axis in space on the elastic vibration pattern is formulated. The effect of cross-coupling between eigenmodes in the system with the same number of parallel nodes but different number of meridional nodes, i.e., the precessing harmonic vibration wave, is analyzed and the problem of eigenvector and eigenvalue perturbations of the vibration equation is considered. The findings indicate that the random nature of the angular velocity direction vector of the elastic body introduces correction only for eigenvectors while the coefficient characterizing the wave precession does not change. References 5.

On Theory of Elastoplastic Superconducting Shell Reliability

937F0086G Moscow IZVESTIYA AKADEMII NAUK: MEKHANIKA TVERDOGO TELA in Russian No 4, Jul-Aug 92 pp 135-150

[Article by Ye.V. Lobanov, Moscow; UDC 539.3]

[Abstract] The considerable mechanical stresses developing in superconducting shells in such devices as tokamak magnetic systems and the difficulty of assessing the limiting state of such structures prompted a study of the theory of reliability of elastoplastic homogeneous isotropic superconducting shells on the basis of the principle of linearizing the physically and geometrically nonlinear equations of the theory of superconducting shells against the background of an elastoplastic zero-moment state. To this end, a closed system of equations of superconducting shells is derived on the basis of L.I. Sedov's variational principle. The contravariant components of the medium point velocities, the covariant components of the metric tensor, and entropy mass density, the covariant components of the electric field strength and other functions are used as the defining parameters of the superconducting shell. The theory of random scalar field overshoots is used for assessing the survival probability of the elastoplastic superconducting shell in a random field force and the reliability function of the shell under the effect of space-time random forces is derived. References 19: 18 Russian, 1 Western.

Stability of Sectional Composite Cylindrical Shell Under External Pressure

937F0086H Moscow IZVESTIYA AKADEMII NAUK: MEKHANIKA TVERDOGO TELA in Russian No 4, Jul-Aug 92 pp 151-156

[Article by A.V. Lopatin, Krasnoyarsk; UDC 539.3:534.1]

[Abstract] The problem of stability of a sectional composite cylindrical shell made from two parts—one solid and one three-layered—under the effect of external pressure is considered for a specific application as the hull of an underwater device whose operating conditions require that a certain center of gravity position be maintained. The median surface of the shell is studied in a curvilinear system of coordinates whose origin is placed in the joint between two parts of the cylinder. The problem is solved using the equations of the theory of zero-moment cylindrical composite shells and a system of equations in displacements is derived. The boundary

conditions on the shell faces are examined and a uniform system of differential algebraic equations is derived. The approach to solving the stability problem of the composite sectional shell is realized as a computation routine and the method of division in half is used to find the roots of the equation. The eigenvalues and eigenvectors are calculated by the double iteration method. The critical pressure value for a shell with specific parameters is determined for illustrations. Figures 2; references 3.

Mathematical Modeling of Straining Dynamics of Multifold Solar Battery During Deployment

937F0086I Moscow IZVESTIYA AKADEMII NAUK: MEKHANIKA TVERDOGO TELA in Russian No 4, Jul-Aug 92 pp 183-190

[Article by V.I. Panichkin, Moscow; UDC 624.07:534.1]

[Abstract] The dynamic model of a multifold deployable solar battery (SB) where the folds are located on an elastically strained cross beam rigidly braced to the spacecraft (KA) when deployed is considered. In the proposed dynamic model, the system of solar battery panels is simulated by a planar rod structure whose rod cross section is equal to the cross section area of two thin-walled carbon plastic frame tubes while their mass is assumed to be equal to the mass of the solar battery panels. The rod system straining equations are derived through the planar equations of motion, force-strain constraint equations, and strain-displacement correlations. Godunov's method is used for examining the dynamic process in the rod system and the solution algorithm is described. For illustration, the algorithm for calculating one time step in the mathematical model is analyzed in detail. It is noted that since there are no precise analytic solutions of such problems and experimental data of structural tests are still rather tentative, the algorithm had to be checked using a system with four panels with a stationary root section. The smallness of rod deformation made it possible to regard the panel motion produced by two dynamic models to be close enough. Calculations confirm this assumption. Figures 7; references 10: 9 Russian, 1 Western.

Calculating Operational Dimensions in a Production Technology CAD System

937F0082G Leningrad IZVESTIYA VYSSHIKH UCHEBNYKH ZAVEDENIY: PRIBOROSTROYENIYE in Russian No 9, Sep 92 (manuscript received 6 Mar 91) pp 91-98

[Article by D.D. Kulikov and M.V. Dygina, Leningrad Institute of Precision Mechanics and Optics; UDC 621.3-523.8:658.512/513]

[Abstract] A new method is proposed for calculating operational dimensions when designing production technology. The new method, which is based on the use of production technology CAD systems, is an improved version of the Tsep CAD subsystem that was developed for use with SM-4 computers. In the original Tsep system, manufacturing processes could only be designed after all of the operations had already been designed and after dimensioning had been performed for all operations involved in the given process. Then, after having designed the given manufacturing process at the route level, users of the Tsep system had to return to the process of designing the individual operations and then to planning the transfers between operations (i.e., to designating cutting and measuring tools based on the calculated manufacturing dimensions). This need to finalize the designs of operations and transfers lengthened the design process considerably because changes in the dimensioning of bases and in the manufacturing dimensions achieved in one operation might necessitate the redesign of operations already designed. In the revised Tsep system, the calculations involved in designing a manufacturing process were shifted from the route level to the level of operations and transfers between them. This was accomplished by implementing the design process from the final operation to the initial operation. The graph of final dimensions is formulated as operations are designed, and the allowances removed in individual operations are added to the graph. The graph of intermediate process dimensions is also compiled in the same sequence. Only those process dimensions actually achieved are added to the graph of intermediate process dimensions. Test calculations confirmed the validity of this approach, and the appropriate algorithms and software were developed. A test of the operation of the revised Tsep system established that shifting the focus of the design process from the route level to the operation and interoperation transfer level as in the new version of the Tsep production technology CAD system permits the timely discovery of errors related to incorrect base selection and dimensioning, as well as significantly reduces the number of operations that must be redesigned and thus reduces the overall time required to design a manufacturing process. Figures 6, tables 2; references 3 (Russian).

Contactless Radio Wave Methods of Measuring Electrophysical Parameters of Semiconductor Materials

937F0066A Tomsk IZVESTIYA VYSSHIKH UCHEBNYKH ZAVEDENIY: FIZIKA in Russian No 9, Sep 92 pp 45-63

[Article by M.V. Detinko, Yu.V. Lisyuk, Yu.V. Medvedev, A.A. Skrylnikov, Siberian Engineering Physics Institute imeni V.D. Kuznetsov at the Tomsk State University; UDC 621.3.083.2-52:537.311.322]

[Abstract] The requirements to measure the electrophysical parameters of semiconductor materials at the growth stage, and of integrated circuits at the fabrication stage, by contactless nondestructive methods which preserve the surface stability of the sample, have a high spatial resolution, are capable of measuring several parameters simultaneously, have a high output, and are at least as accurate as the four-probe methods are summarized and it is noted that radio wave methods (within a 100 kHz to 1 GHz band) meet the above requirements most fully. A number of promising contactless methods of nondestructive testing with the help of quasistationary resonant transducers whose probing electromagnetic field is clearly spatially localized within the small volume of the item under study are considered and numerous publications are reviewed. The principles of measuring the semiconductor resistivity by the quasistationary resonator, the design of microwave resonators used as electrophysical parameter transducers, methods of designing resonator-type transducers, contactless semiconductor wafer and structure diagnostics by the microwave magnetoresistance method, microwave magnetoresistance of a semiconductor wafer in a uniform SHF electric field, and other specific aspects of the problem are outlined in detail. Appropriate working frequency selection makes it possible to combine high spatial resolution with sufficient conversion transconductance for materials with a broad range of resistivity (10^{-3}-10^{9} Ω x cm). It is speculated that the advantages of the method will make it possible to extend its applications to multilayer structure diagnostics, doping profile measurements, etc. Figures 10; references 52: 49 Russian, 3 Western.

END OF FICHE DATE FILMED

12 February 1993